

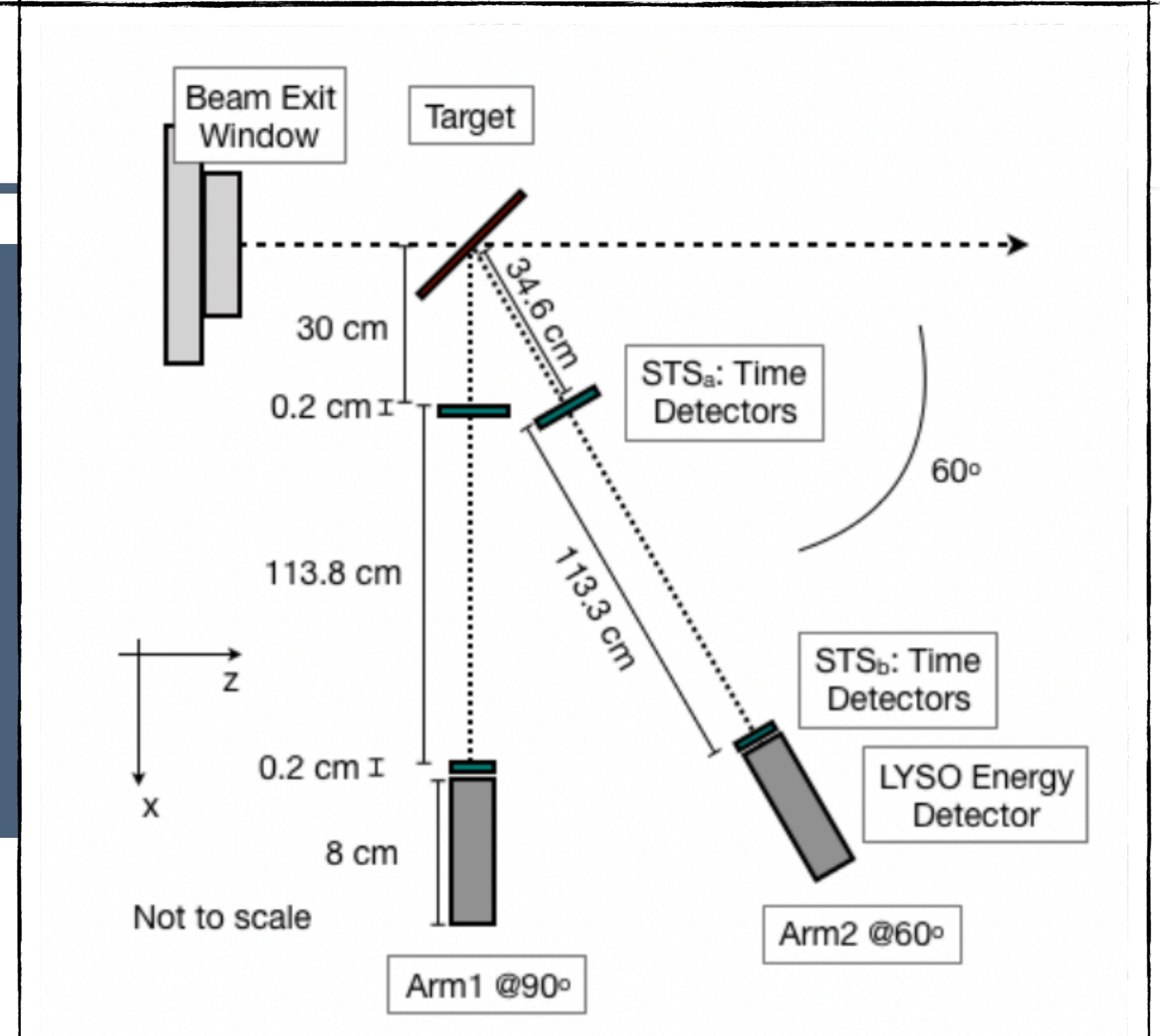
# Measurement of charged fragments production cross sections ( $d\sigma/dE$ ) in the interactions of C-ions with C,H,O targets

CNAO July 2017 Data Taking

# Experimental Setup

- 3 thin targets (1-2 mm) based on C, H, O elements  
**PMMA, C, CH**
- 3 detection angles:  $90^\circ$ ,  $60^\circ$ ,  $32^\circ$
- 5 Carbon Ion beam energies:  
**115, 150, 221, 279, 351 MeV/u**

- Fragments production ( $Z=1$ ,  $A = 1, 2, 3$ ) as a function of the production kinetic energy
- Time of Flight in thin plastic scintillators and energy deposit in the inorganic crystals for PID and  $E_{kin}$  measurements
- Experimental Data - Monte Carlo simulation comparison



4 STSs 2mm thick for ToF measurement (time resolution  $\sim 400-600$  ps) and Deposited Energy measurement (dE);  
2 LYSOs  $4 \times 4 \times 8$  cm<sup>3</sup> for Deposited Energy measurement (E);

# Cross Section Formula

---

The  $^{12}\text{C}$  fragmentation cross section for a  $^A_Z X$  fragment are obtained as:

$$\frac{d\sigma}{dE_k} \left( \begin{smallmatrix} A \\ Z \end{smallmatrix} X \right) = \frac{N_{\begin{smallmatrix} A \\ Z \end{smallmatrix} X}(E_k)}{\Delta E_k} \cdot \frac{\textit{purity}(E_k)}{N_{12C} N_Y} \cdot \frac{1}{\epsilon}$$

# Cross Section Formula: Normalization

The  $^{12}\text{C}$  fragmentation cross section for a  $^A_Z X$  fragment are obtained as:

$$\frac{d\sigma}{dE_k} \left( ^A_Z X \right) = \frac{N_{^A_Z X} (E_k)}{\Delta E_k} \cdot \frac{\text{purity}(E_k)}{N_{^{12}\text{C}} N_Y} \cdot \frac{1}{\epsilon}$$

From CNAO  
Dose Delivery System

Information on the target  
composition:

dose-current conversion systematic uncertainty. The relative uncertainty on  $N_{^{12}\text{C}}$  (4%) is hence the convolution of the uncertainty on the stopping power determination [20] and on the dose measurements [21]. A possible additional contribution to the systematic uncertainty, coming from the monitoring system measurement stability [22], was found to be negligible

Target	Composition	Thickness [mm]	Density [g/cm <sup>3</sup> ]
PMMA	C <sub>5</sub> O <sub>2</sub> H <sub>8</sub>	2	1.19
Graphite	C	1	0.94
Plas.Scint.	C <sub>b</sub> H <sub>a</sub>	2	1.024

$$N_Y = \frac{\rho_Y \cdot th_Y \cdot N_A}{A_Y}$$

$$th_Y = th_Y \cdot \text{sqrt}(2)$$

$N_{^{12}\text{C}}$	$\cdot 10^6$	$\cdot 10^6$	$\cdot 10^6$	$\cdot 10^6$	$\cdot 10^6$
Target	115 [MeV/u]	153 [MeV/u]	222 [MeV/u]	281 [MeV/u]	353 [MeV/u]
PMMA	49866	46512	49395	49601	42000
Graphyte	49454	46583	47484	47288	49328
Plast. Scint.	49728	50600	49347	49787	49653

# Cross Section Formula: Yield

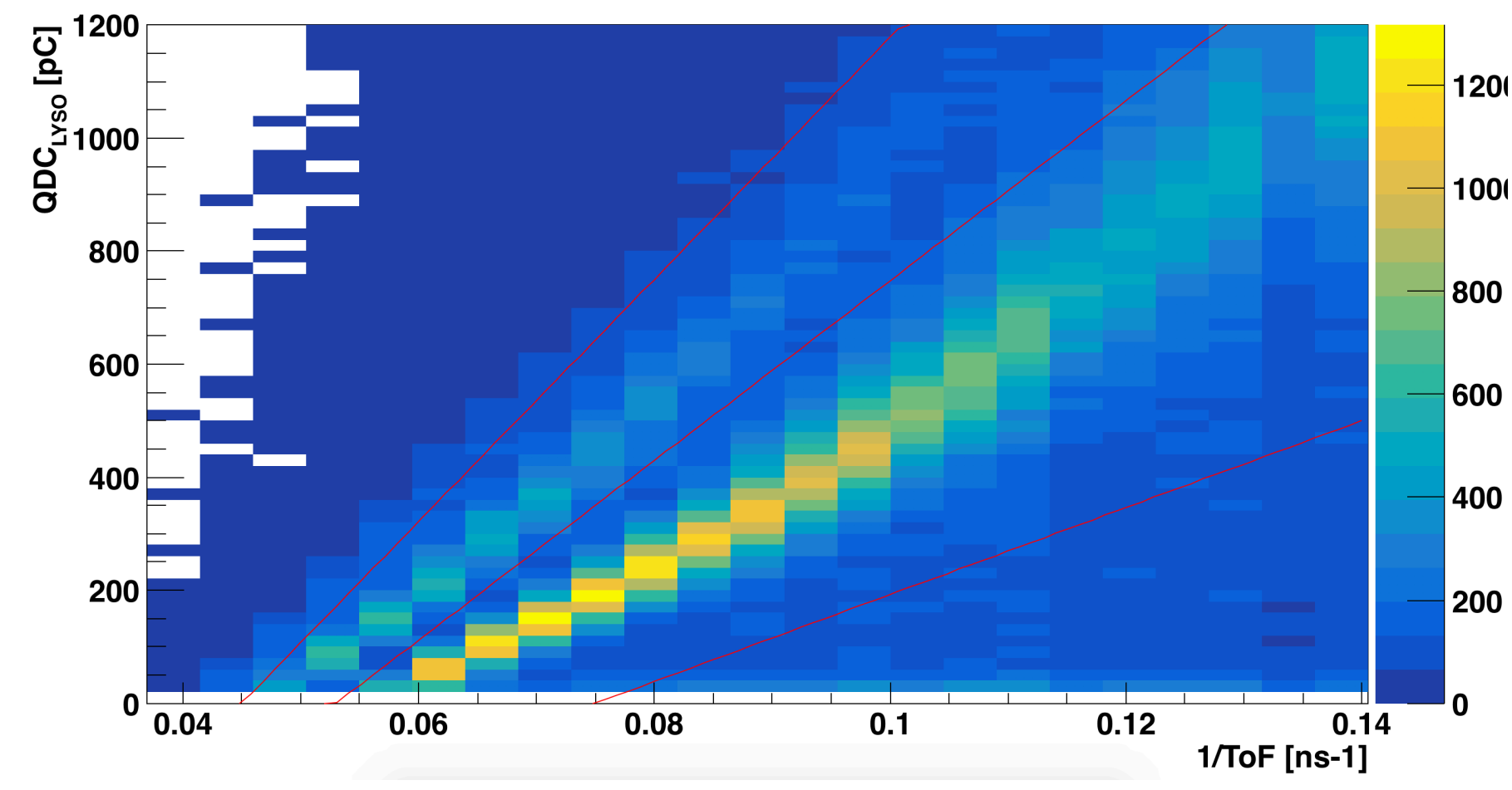
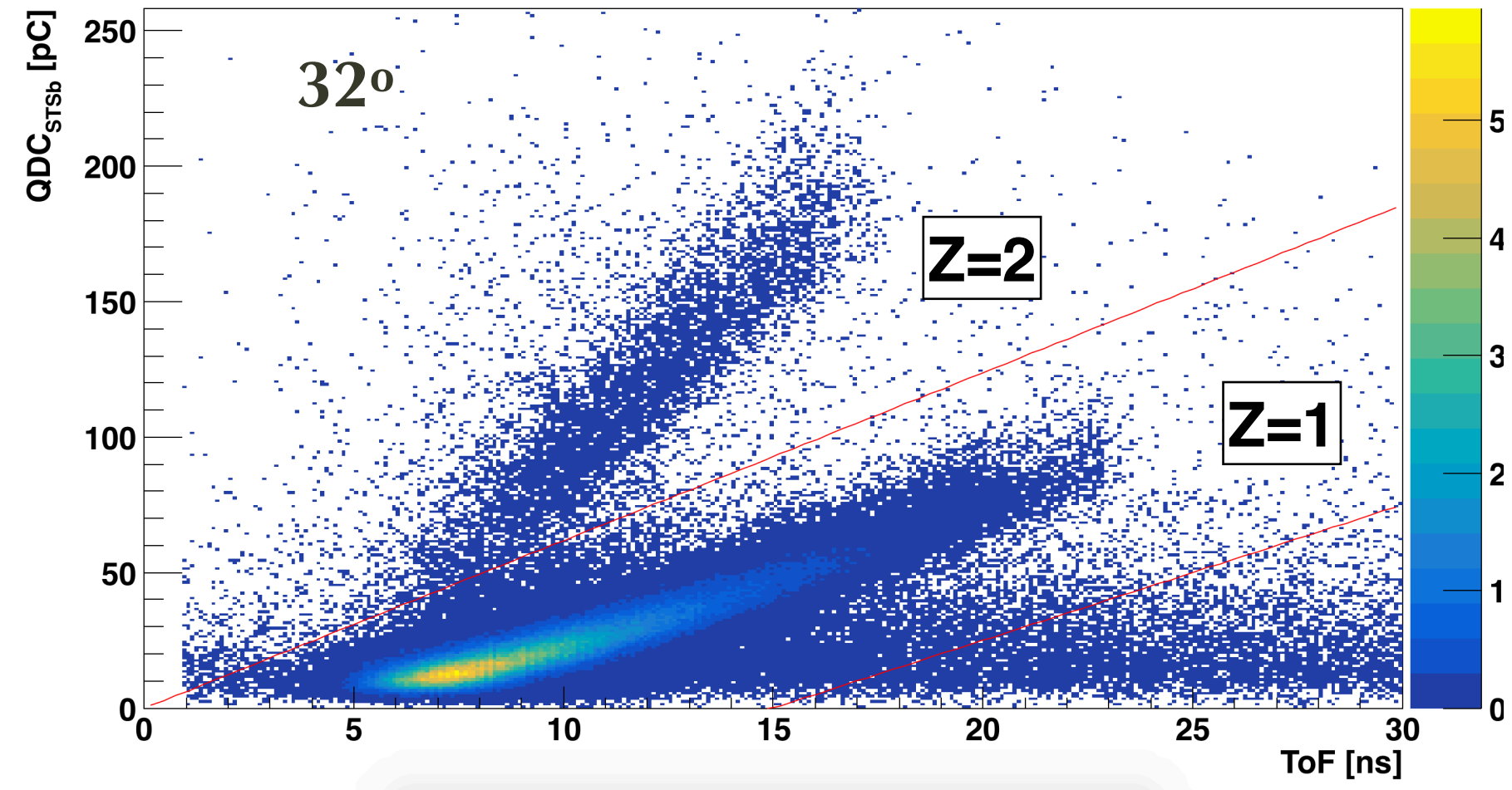
$$\beta_i = L / (ToF_i \cdot c)$$

$$E_{kin} = m_i \cdot (\gamma - 1)$$

The  $^{12}\text{C}$  fragmentation cross section for a  $^A_Z X$  fragment are obtained as:

$$\frac{d\sigma}{dE_k} \left( ^A_Z X \right) = \frac{N_{A_Z X}(E_k)}{\Delta E_k} \cdot \frac{purity(E_k)}{N_{12C} N_Y} \cdot \frac{1}{\epsilon}$$

- Particle identification (Z,A) from combining the information of QDC LYSO, QDC STSs, ToF STSs



# Cross Section Formula: Yield

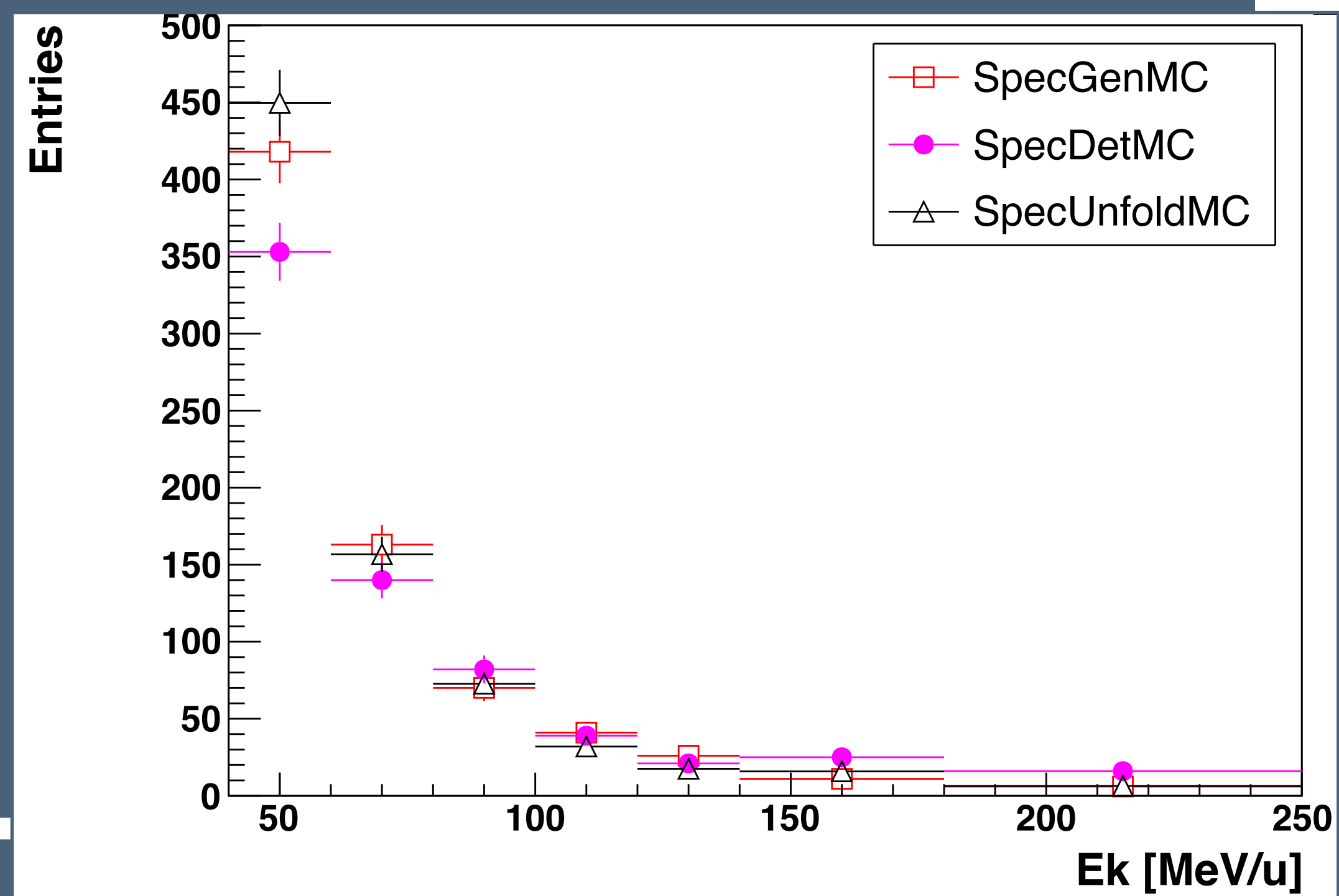
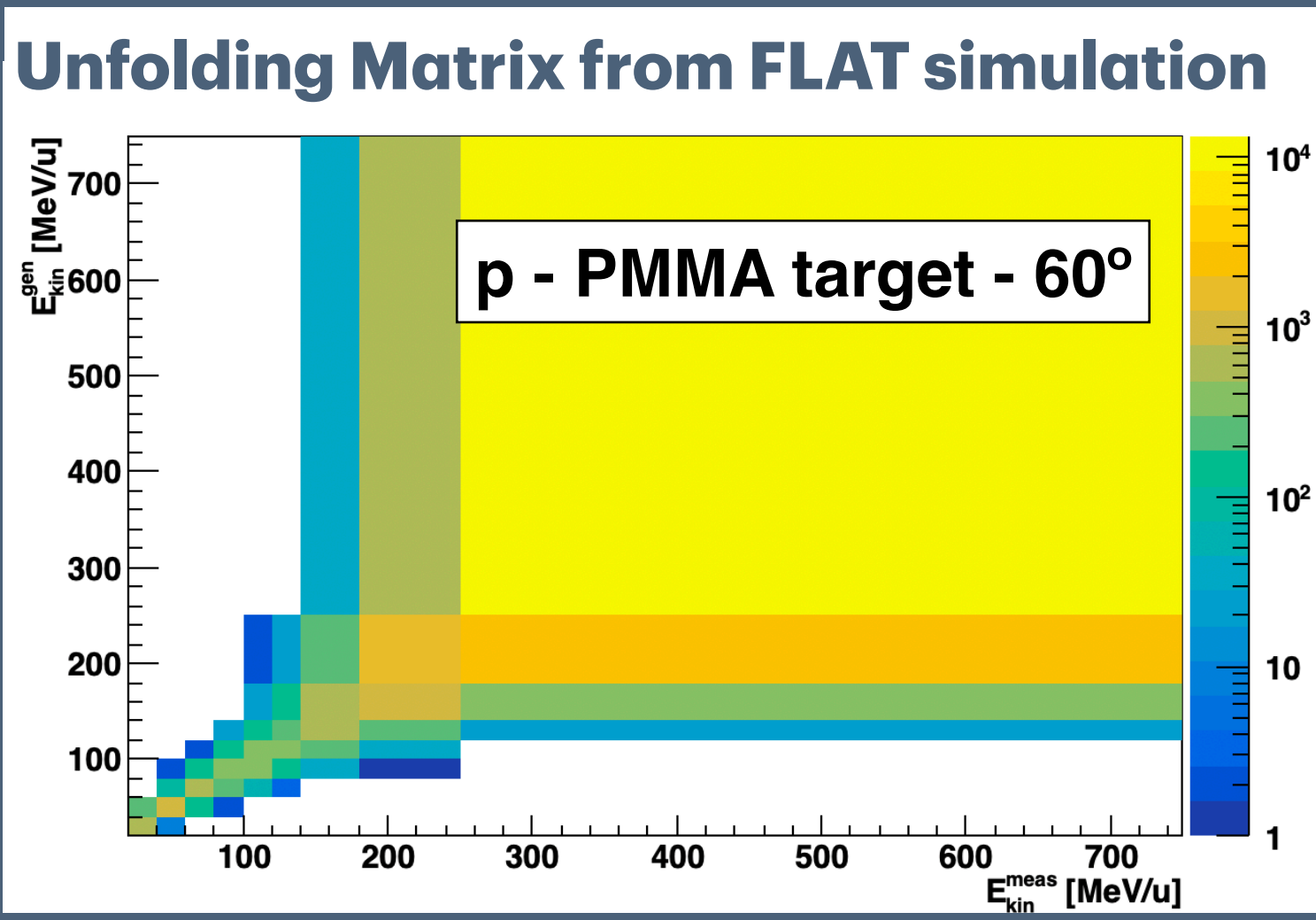
$$\beta_i = L / (ToF_i \cdot c)$$

$$E_{kin} = m_i \cdot (\gamma - 1)$$

The  $^{12}\text{C}$  fragmentation cross section for a  $^A_Z X$  fragment are obtained as:

$$\frac{d\sigma}{dE_k} \left( ^A_Z X \right) = \frac{N_{A_X}(E_k)}{\Delta E_k} \cdot \frac{purity(E_k)}{N_{12C} N_Y} \cdot \frac{1}{\epsilon}$$

- Unfolding technique (RooBayesUnfold) to obtain the fragments  $E_{kin}^{gen}$  from  $E_{kin}^{meas}$



# Cross Section Formula: Purity

$$\beta_i = L / (ToF_i \cdot c)$$

$$E_{kin} = m_i \cdot (\gamma - 1)$$

The  $^{12}\text{C}$  fragmentation cross section for a  $^A_Z X$  fragment are obtained as:

$$\frac{d\sigma}{dE_k} \left( \frac{A}{Z} X \right) = \frac{N_{A_Z X}(E_k)}{\Delta E_k} \cdot \frac{\text{purity}(E_k)}{N_{^{12}\text{C}} N_Y} \cdot \frac{1}{\epsilon}$$

$$\text{Purity} = \frac{\text{number of particles selected as } p \text{ (d,t)}}{\text{number of true } p \text{ (d,t) in } p \text{ (d,t) selection}}$$

# Cross Section Formula: Efficiency

$$\beta_i = L / (ToF_i \cdot c)$$

$$E_{kin} = m_i \cdot (\gamma - 1)$$

The  $^{12}\text{C}$  fragmentation cross section for a  $^A_Z X$  fragment are obtained as:

$$\frac{d\sigma}{dE_k} \left( ^A_Z X \right) = \frac{N_{^A_Z X}(E_k)}{\Delta E_k} \cdot \frac{purity(E_k)}{N_{^{12}\text{C}} N_Y} \cdot \boxed{\epsilon}$$

$$\boxed{\epsilon} = \epsilon_{Det} \cdot \epsilon_{Sel} \cdot \epsilon_{DT}$$

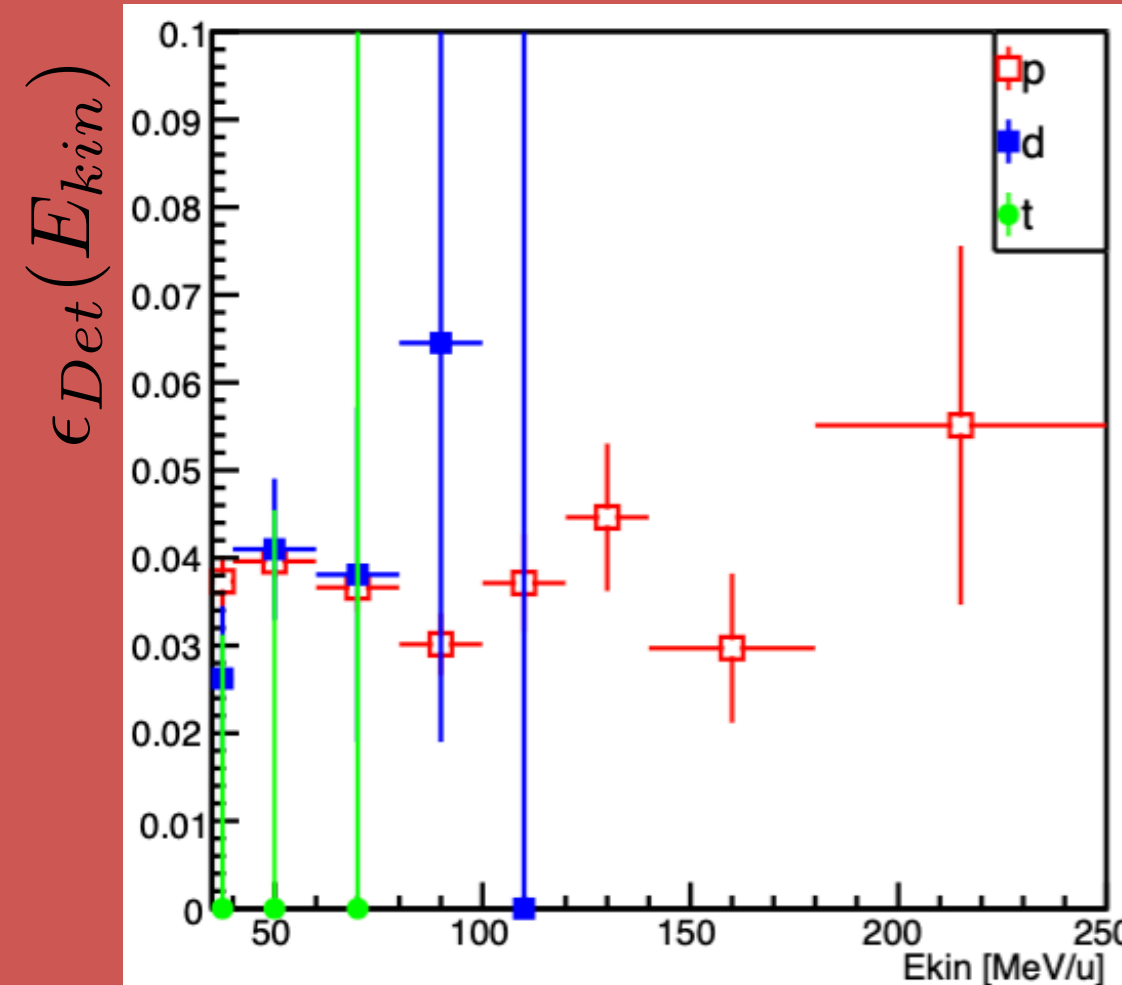
## Full simulation (FLUKA)

(C on Targets  $\sim 1 \cdot 10^{10}$  primaries)

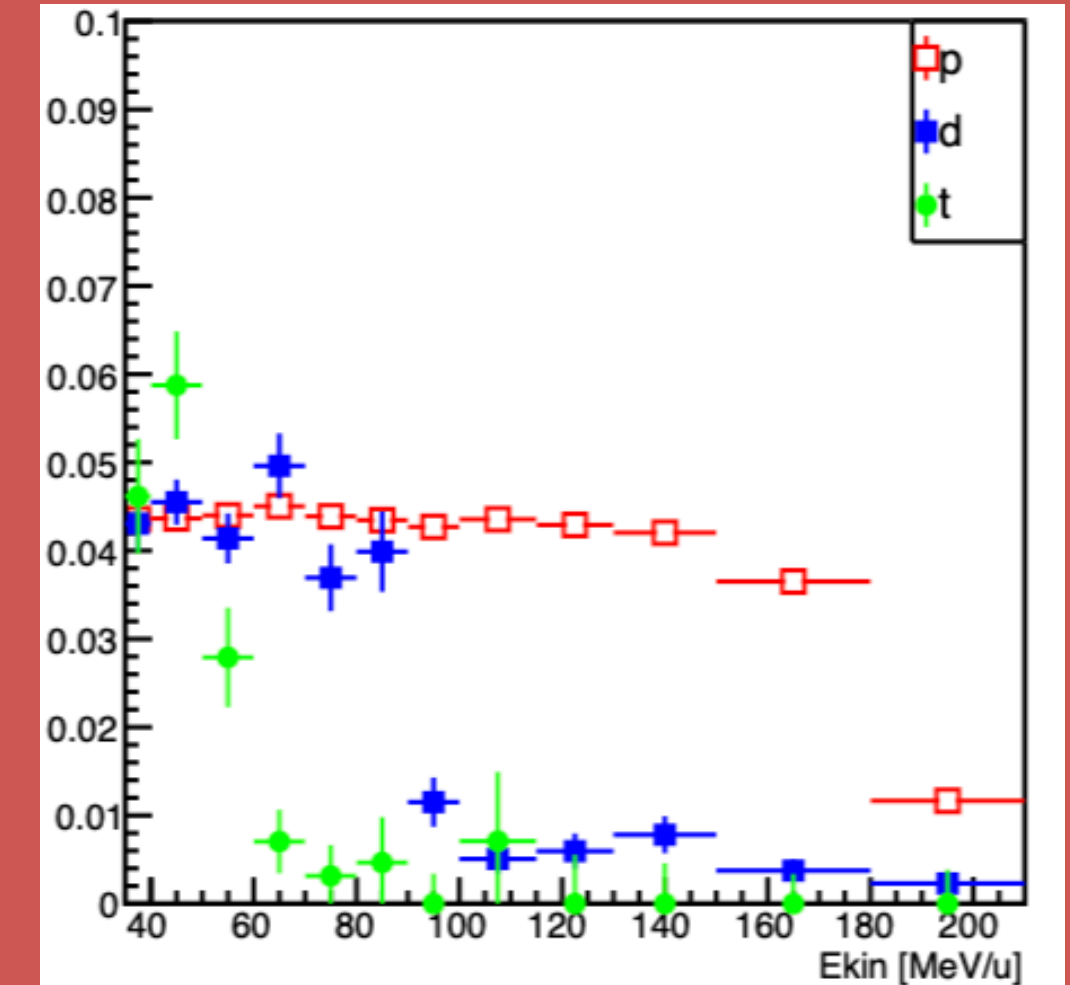
to calculate the

**trigger+detection+geometrical efficiency**  
as a function of fragment production  $E_{kin}$

PMMA target - 90° -  $^{12}\text{C}$  115 MeV/u



PMMA target - 32° -  $^{12}\text{C}$  351 MeV/u





# Cross Section Formula: Efficiency

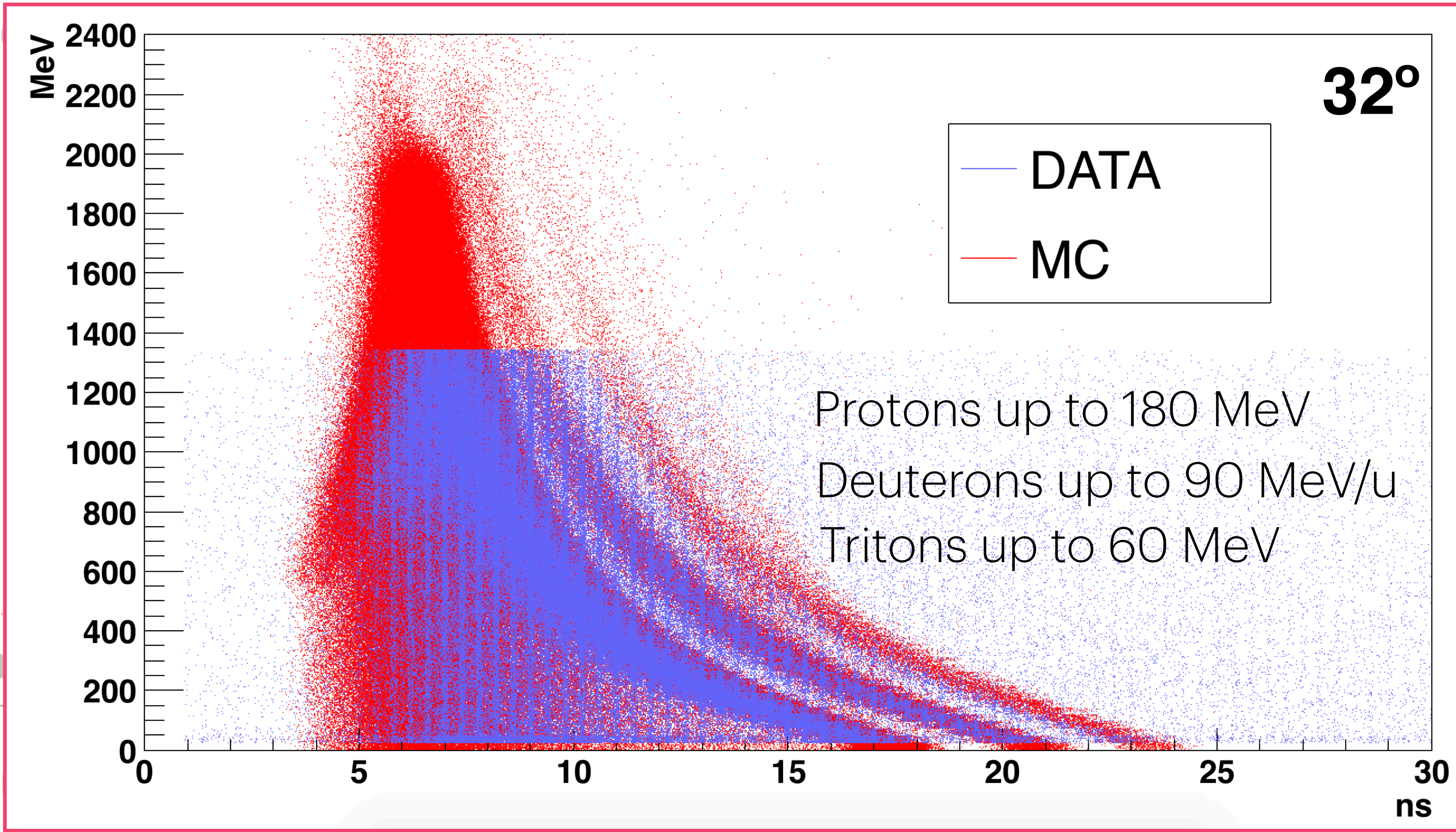
$$\beta_i = L / (ToF_i \cdot c)$$

$$E_{kin} = m_i \cdot (\gamma - 1)$$

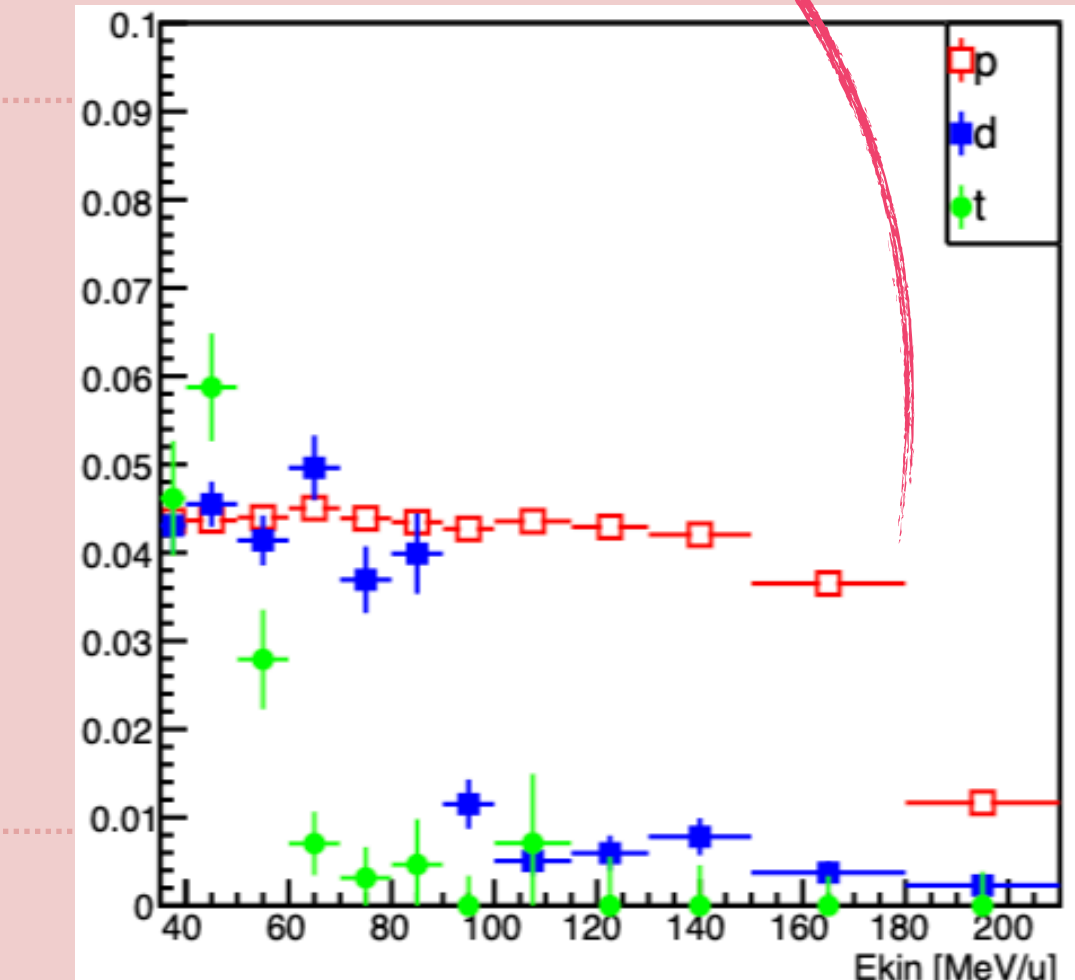
The 12

as:

$$\frac{1}{\epsilon}$$



PMMA target - 32° - <sup>12</sup>C 351 MeV/u



Full sim  
(C on T  
to calc  
trigger+detection+geometrical efficiency  
as a function of fragment production Ekin

# Cross Section Formula: Efficiency

$$\beta_i = L / (ToF_i \cdot c)$$

$$E_{kin} = m_i \cdot (\gamma - 1)$$

The  $^{12}\text{C}$  fragmentation cross section for a  $^A_Z X$  fragment are obtained as:

$$\frac{d\sigma}{dE_k} \left( \frac{A}{Z} X \right) = \frac{N_{A_Z X}(E_k)}{\Delta E_k} \cdot \frac{purity(E_k)}{N_{12C} N_Y} \cdot \boxed{\epsilon}$$

$$\boxed{\epsilon} = \epsilon_{Det} \cdot \epsilon_{Sel} \cdot \epsilon_{DT}$$

**Full simulation (FLUKA)**  
 (C on Targets  $\sim 1 \cdot 10^{10}$  primaries)  
 to compute the **PID efficiency**  
 of PID selection on E (dE) vs ToF  
 distributions, tuned from data

	32° — Ekin [MeV]	$\epsilon_{pp}$ [%]	$\epsilon_{dd}$ [%]	$\epsilon_{tt}$ [%]
PMMA 115	37.5 ± 2.5	97.9 ± 0.3	96.2 ± 0.8	87.4 ± 2.9
	45.0 ± 5.0	98.2 ± 0.2	94.1 ± 0.7	85.7 ± 2.5
	55.0 ± 5.0	98.1 ± 0.2	94.8 ± 0.7	88.0 ± 2.6
	65.0 ± 5.0	96.8 ± 0.3	93.7 ± 0.8	51.6 ± 8.8
	75.0 ± 5.0	96.0 ± 0.4	92.4 ± 0.9	0.0 ± 2.8
	85.0 ± 5.0	95.8 ± 0.4	88.3 ± 1.3	0.0 ± 4.5
	95.0 ± 5.0	95.4 ± 0.4	59.4 ± 4.7	0.0 ± 5.6
	107.5 ± 7.5	94.9 ± 0.4	19.2 ± 5.4	0.0 ± 8.3
	122.5 ± 7.5	93.0 ± 0.6	3.2 ± 3.4	-
	140.0 ± 10.0	90.0 ± 0.7	0.0 ± 3.3	-
	165.0 ± 15.0	80.0 ± 1.2	0.0 ± 8.3	-

# Cross Section Formula: Efficiency

$$\beta_i = L / (ToF_i \cdot c)$$

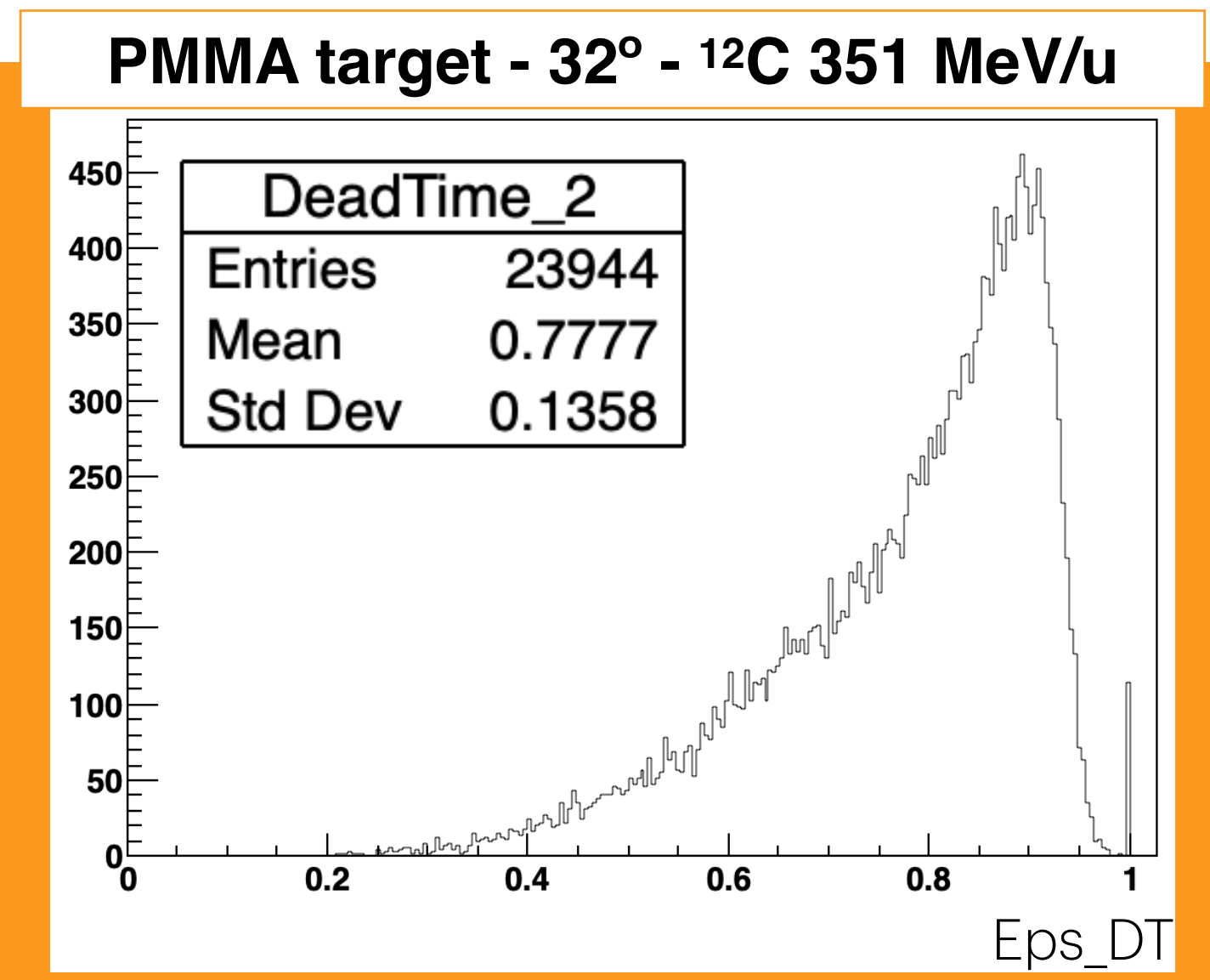
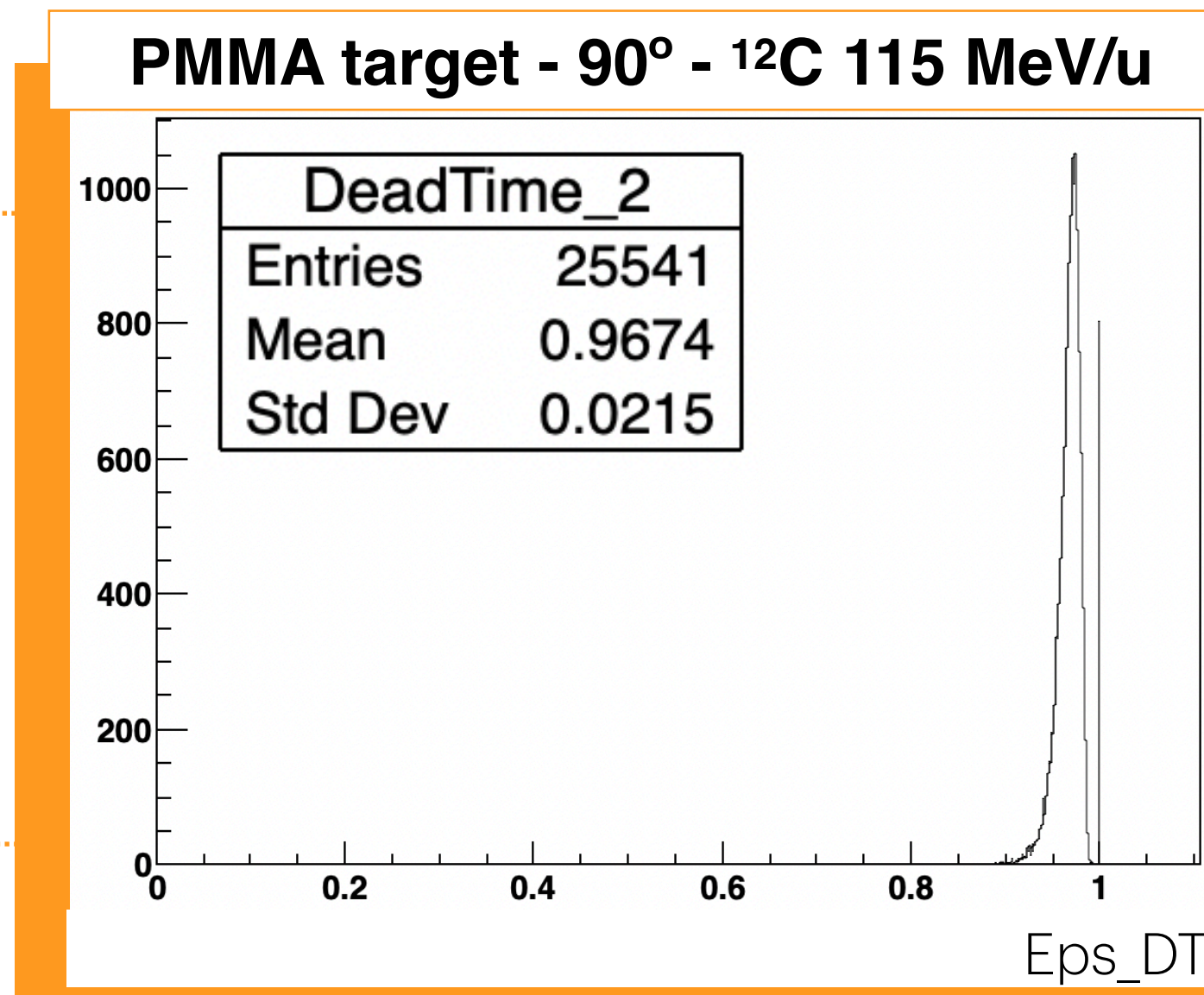
$$E_{kin} = m_i \cdot (\gamma - 1)$$

The  $^{12}\text{C}$  fragmentation cross section for a  $^A_Z X$  fragment are obtained as:

$$\frac{d\sigma}{dE_k} \left( \frac{A}{Z} X \right) = \frac{N_{A_X}(E_k)}{\Delta E_k} \cdot \frac{purity(E_k)}{N_{^{12}\text{C}} N_Y} \cdot \boxed{\epsilon}$$

$$\boxed{\epsilon} = \epsilon_{Det} \cdot \epsilon_{Sel} \cdot \epsilon_{DT}$$

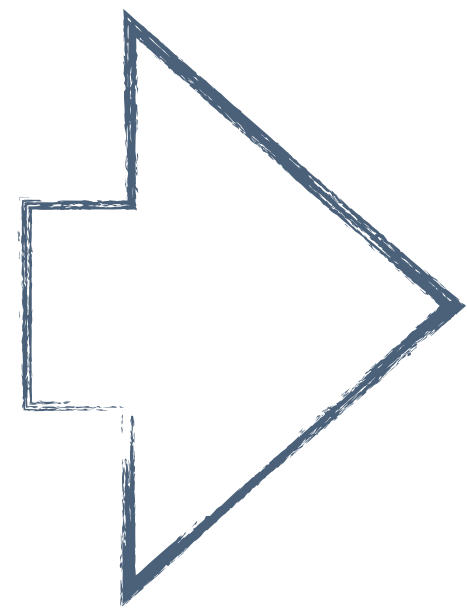
Measurements of the **DAQ dead time** for each run (rate dependent)



# Systematics to the measurement

## 1) Monte Carlo Closure Test:

- study of the Monte Carlo reliability in assessing the efficiencies to be applied to experimental data:
- define the **MCtruth** (EpsDet\_DENO) =  $p(d, t)$ , born in tgt, son of a primary particle, exiting the target, produced in  $(\Theta \pm \Delta\Theta(4^\circ); \varphi \pm \Delta\varphi(4^\circ/6^\circ@32\text{deg}))$  [angular bin due to Multiple Scattering\*]
  - reconstruction of the MC with efficiencies applied (**MCreco**)
  - comparison of MCreco with MC truth



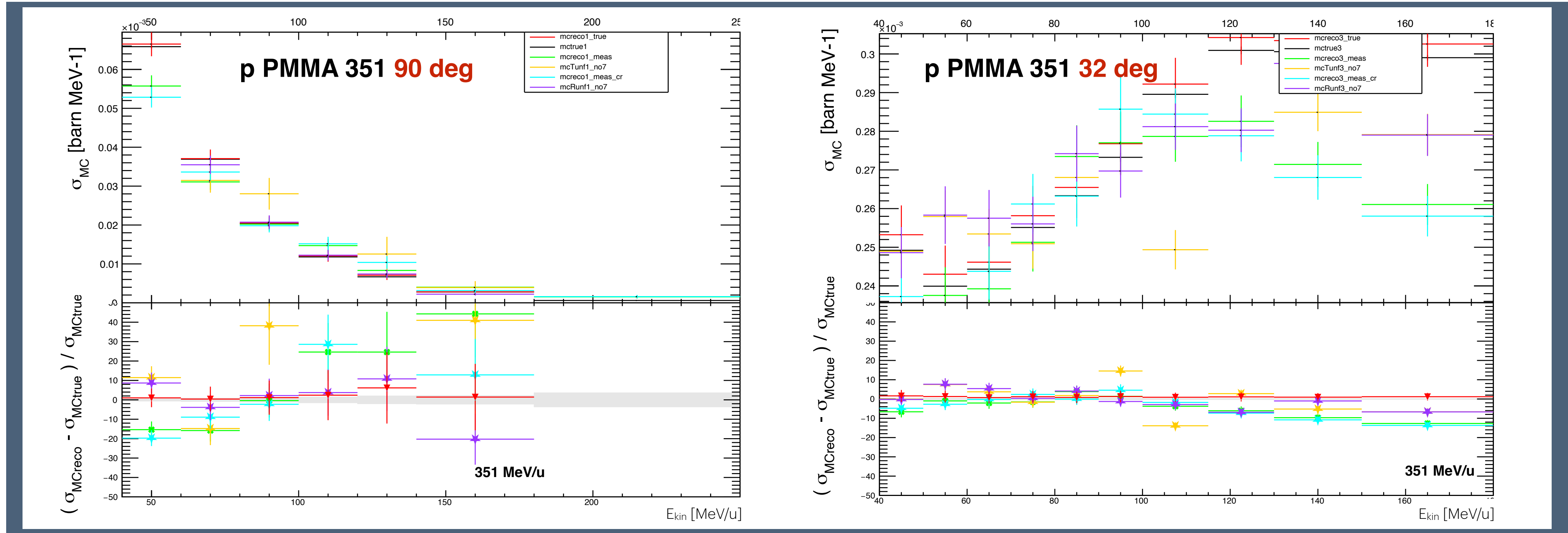
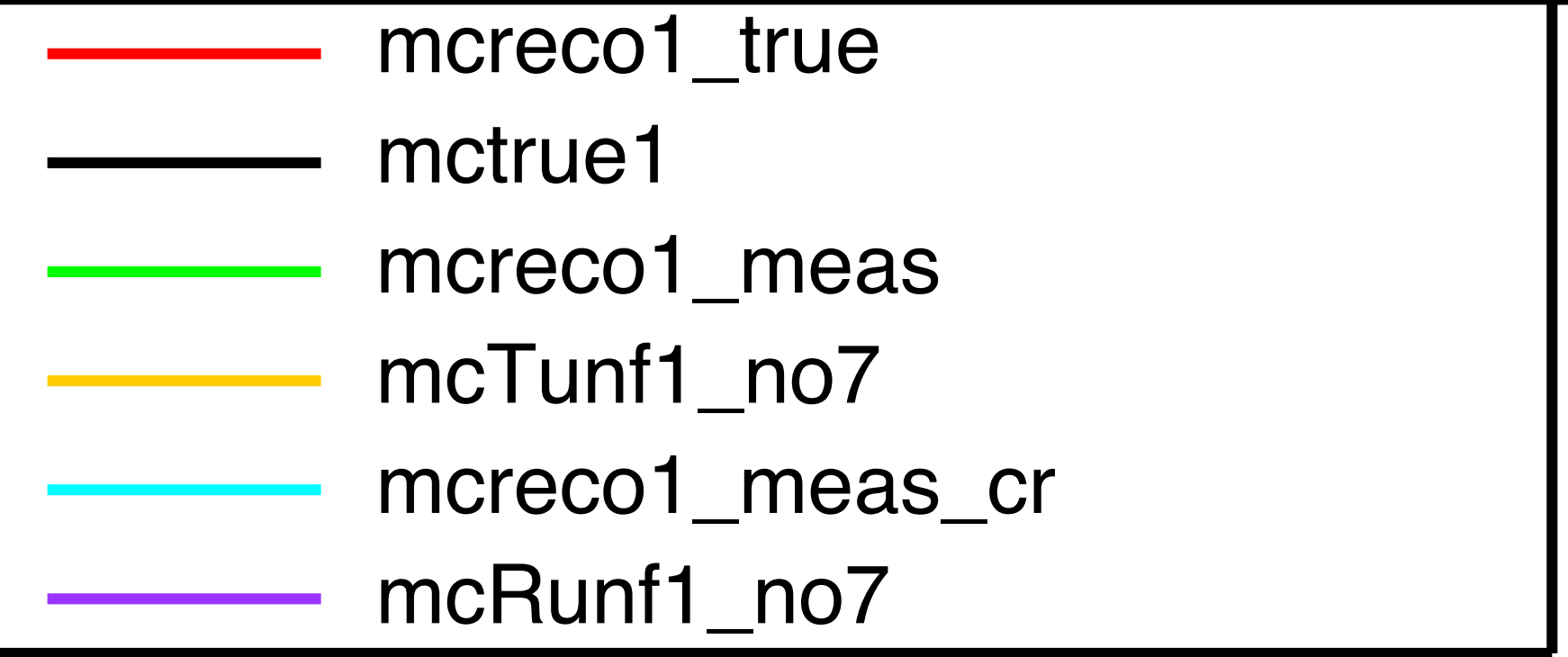
$$\mathbf{sys}_{\text{MC}} = \frac{|\text{MCreco} - \text{MCtruth}|}{\text{MCtruth}}$$

[\*the LYSO theoretical solid angle is  $\Theta, \varphi \pm 0.8^\circ$ ]

# Systematics to the measurement

## 1) Monte Carlo Closure Test:

- **mctrue** = mc @ generation
- **mcreco\_meas** = mc reco (no IDmatch) (Ekin MEAS)
- **mcreco\_true** = mc reco IDmatch (Ekin GEN)
- **mcreco\_meas\_cr** = mc reco IDmatch (Ekin MEAS)
- **mcTunf** = mcreco\_meas UNFOLDED with TUnfold (Ekin@gen)
- **mcRoounf** = mcreco\_meas UNFOLDED with RooUnfold (Ekin@gen)

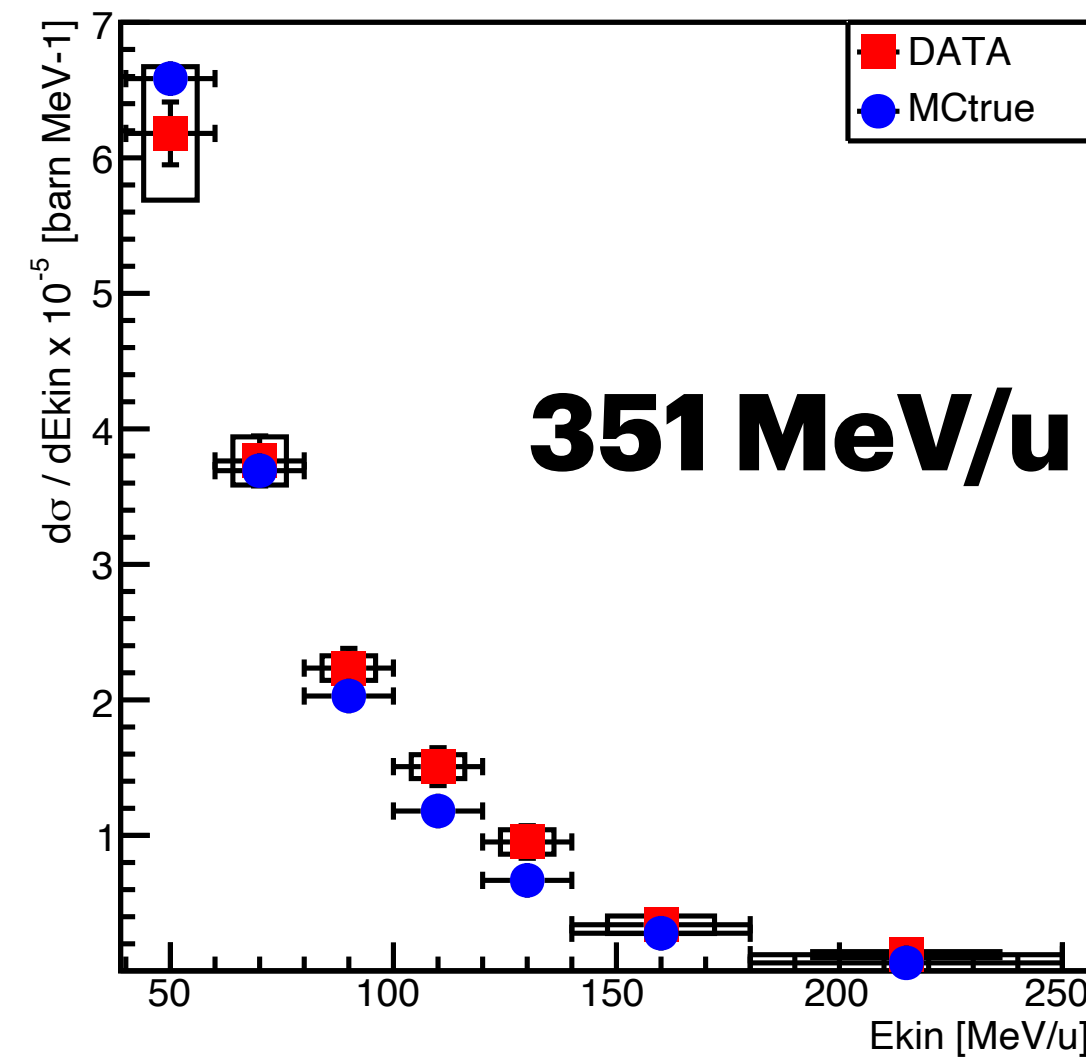
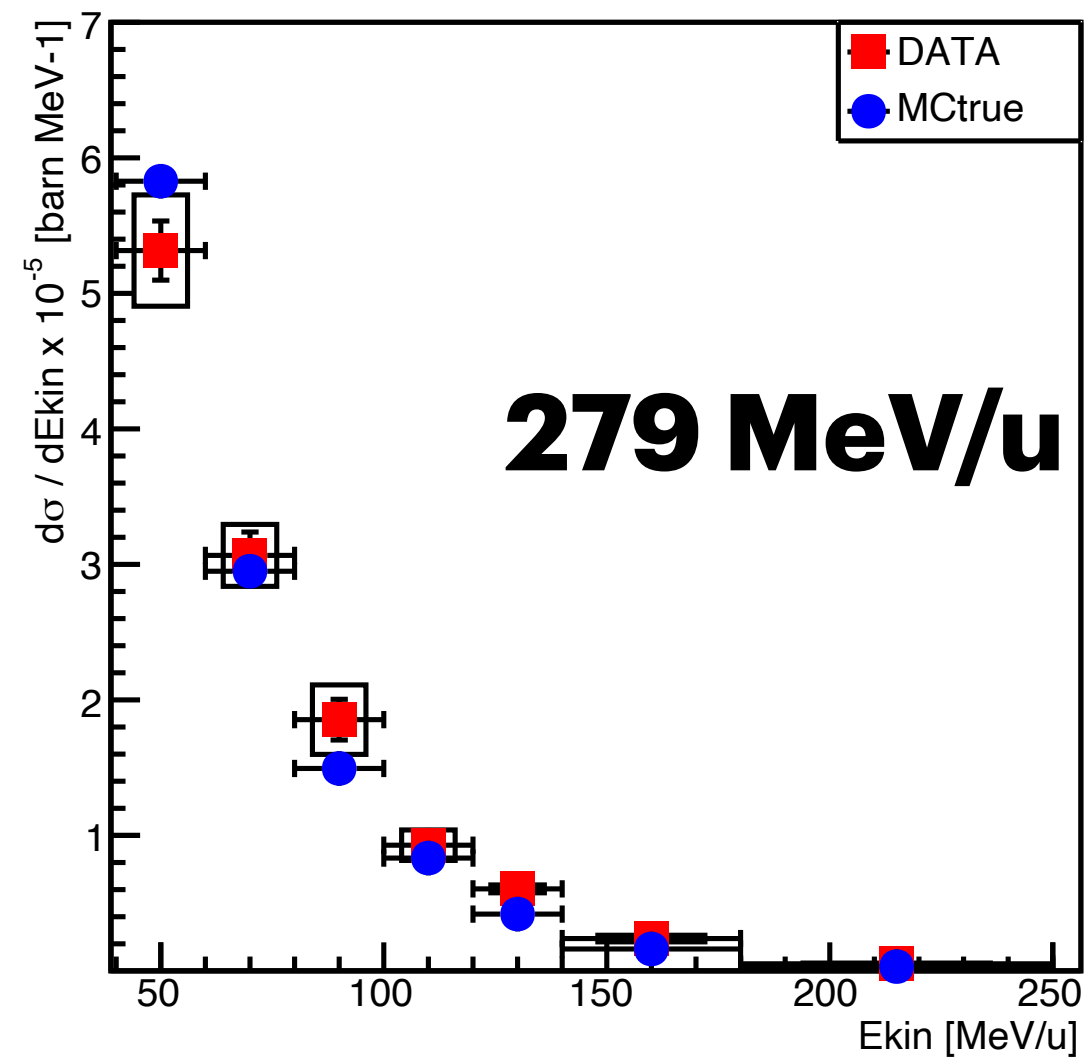
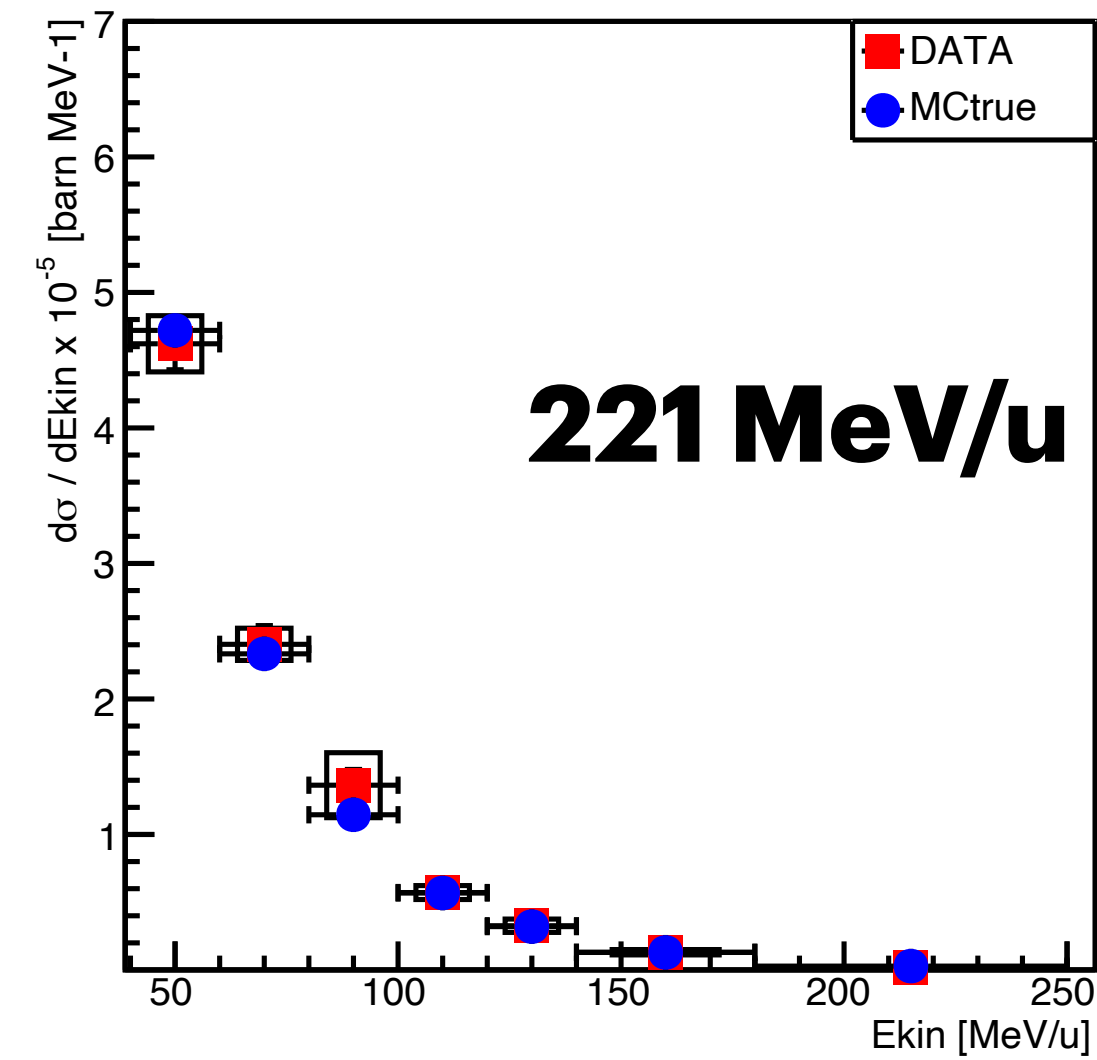
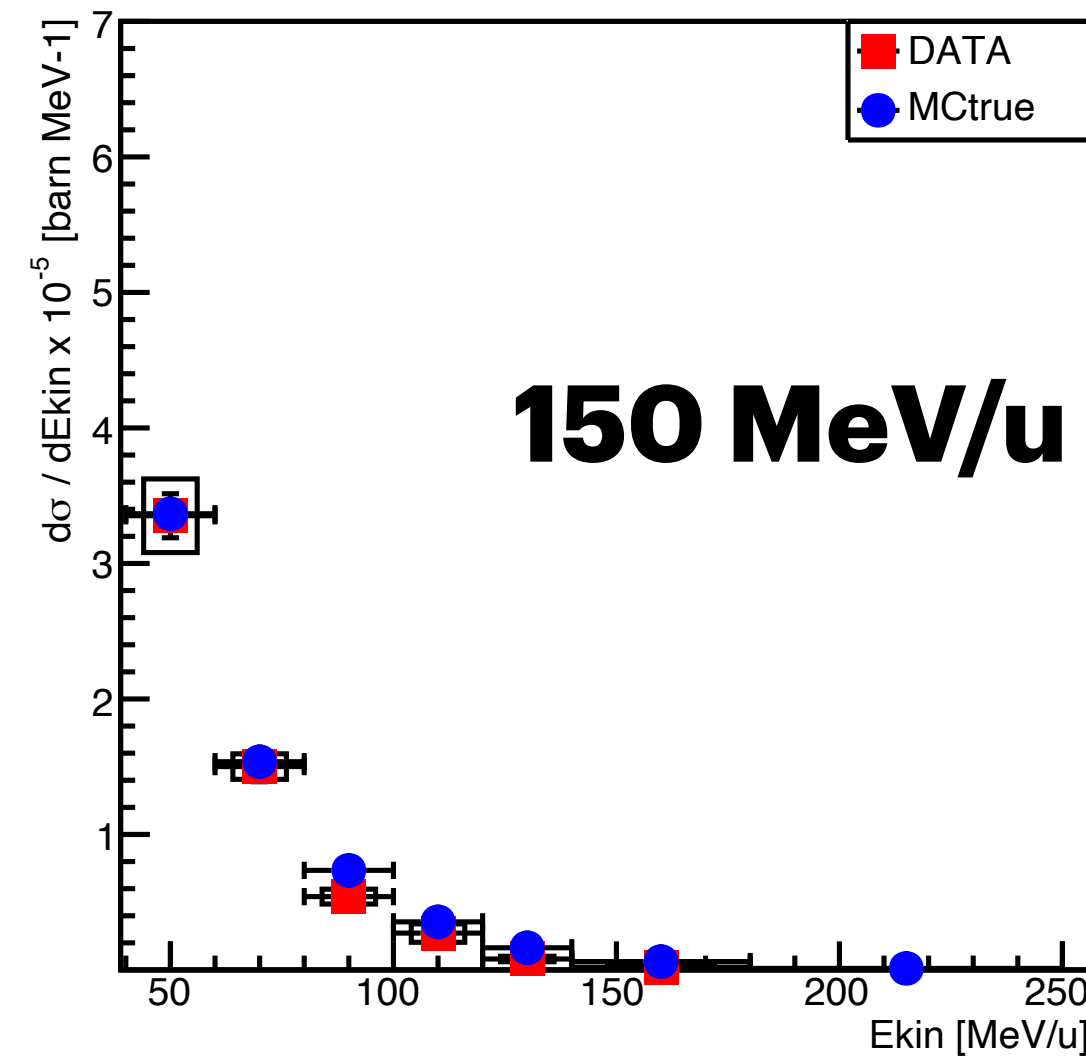
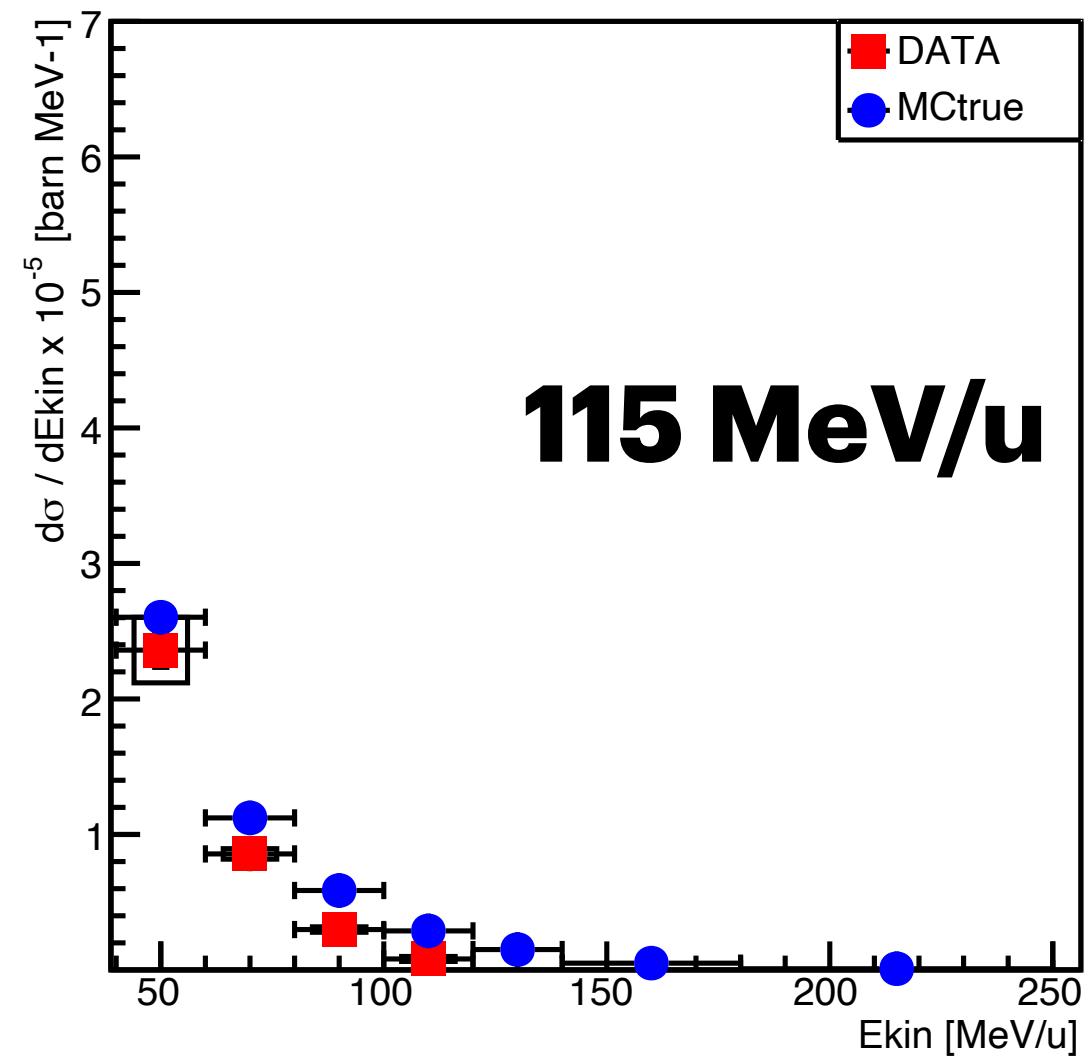


# Systematics to the measurement

---

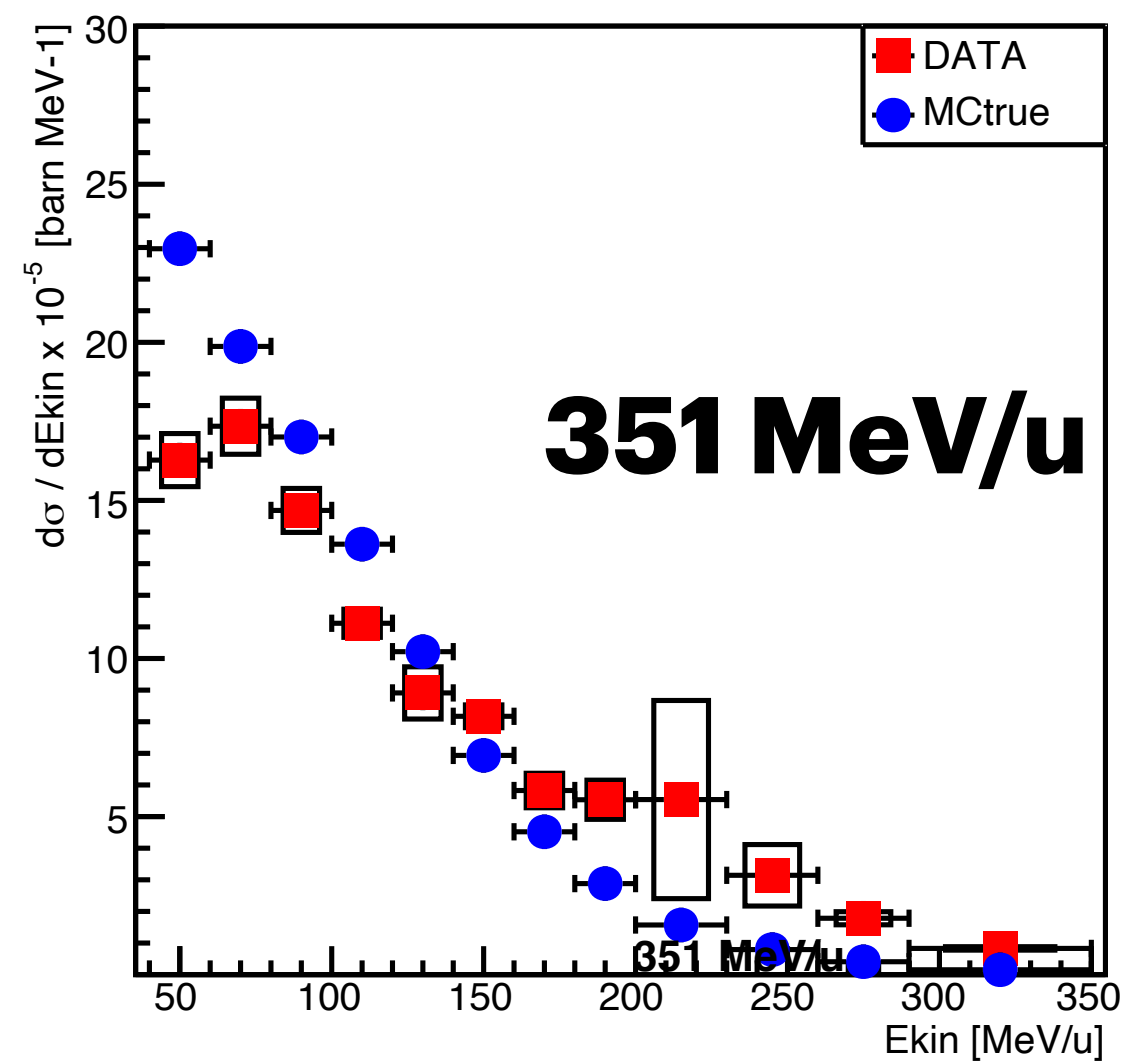
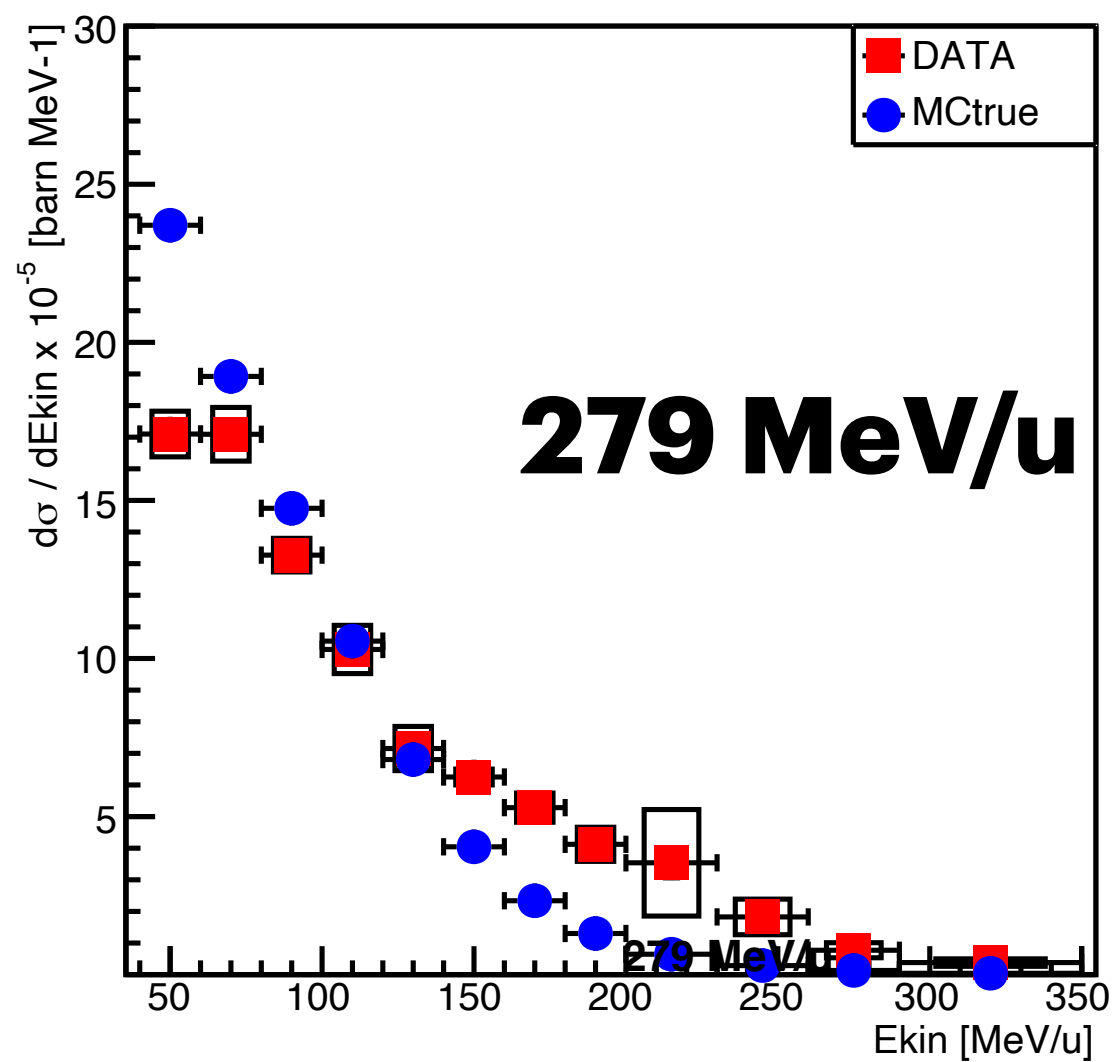
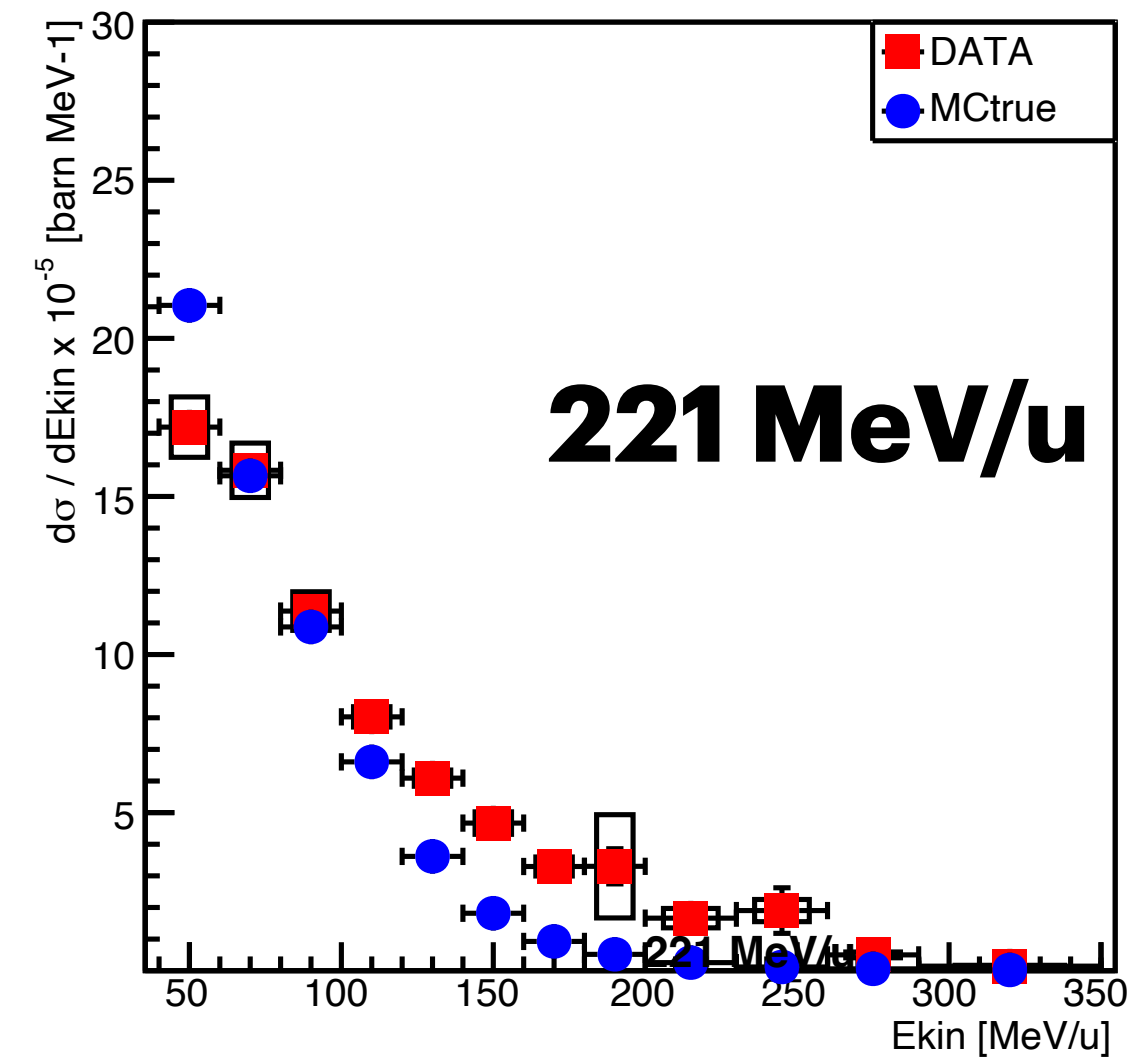
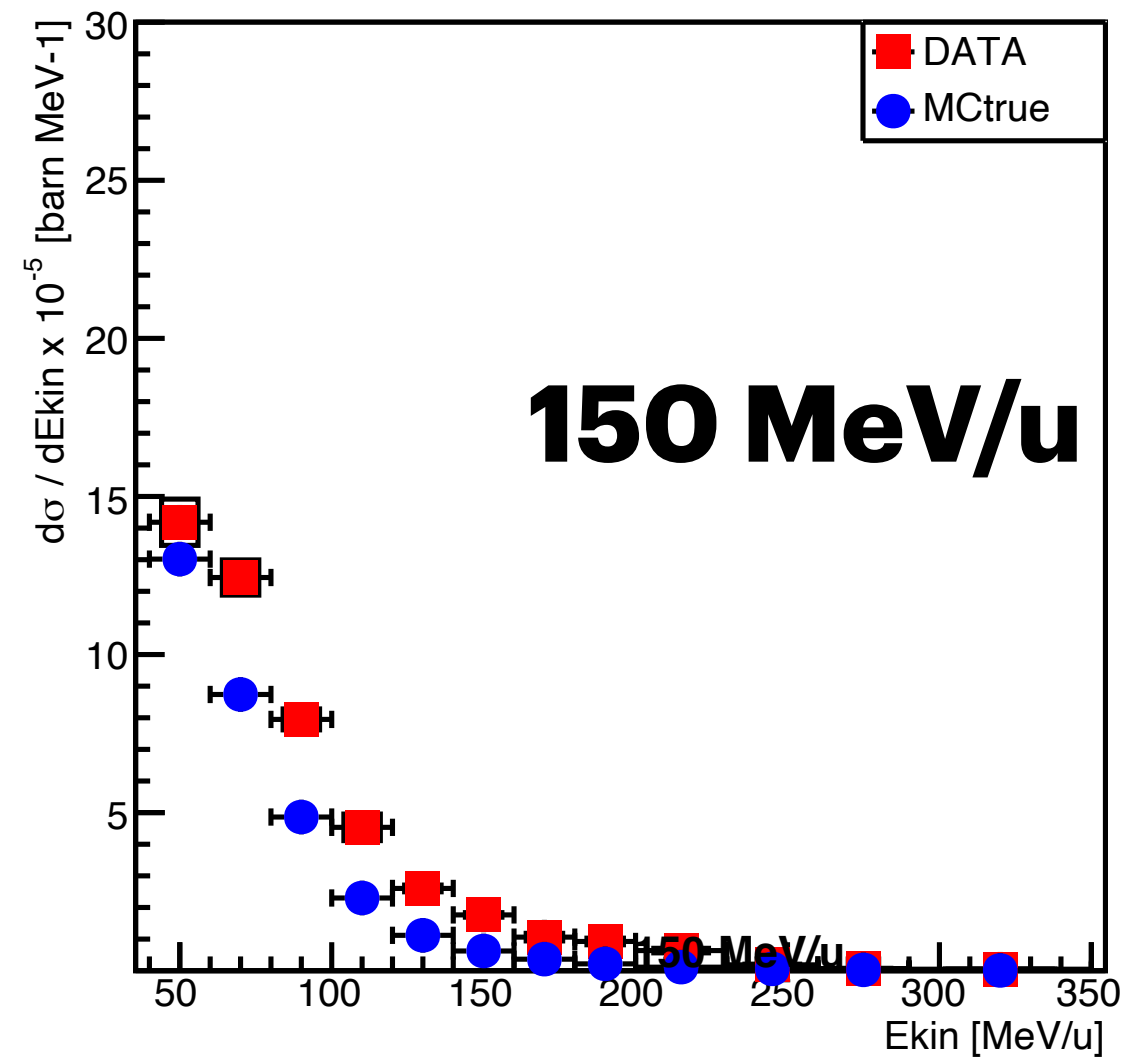
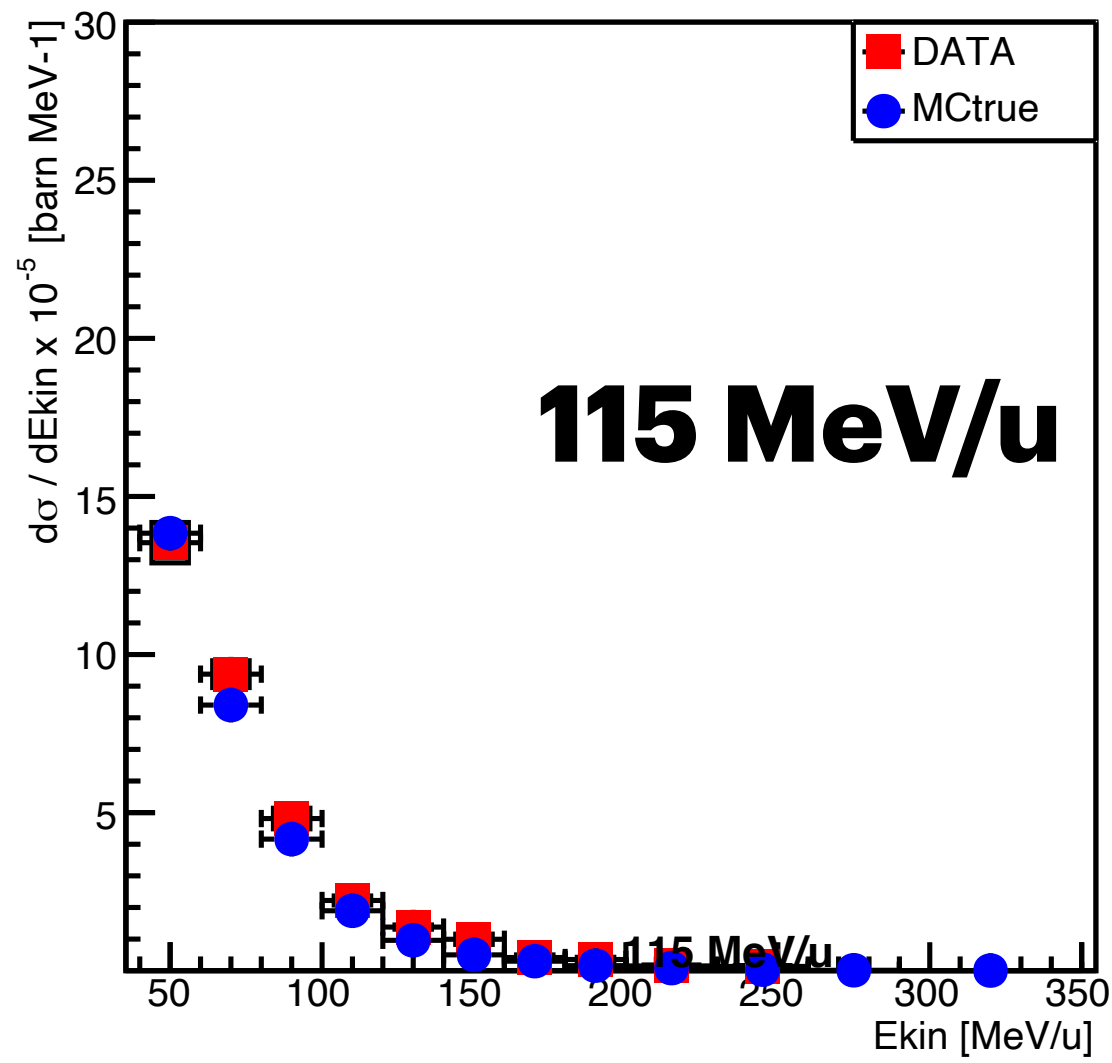
- 2) **PID systematic:** moving the p, d, t selection bands (hard and soft selection) and computing the average difference of XSec wrt the nominal selection ( $\text{sys}_{\text{PID}}$ )
- 3) **EpsDet from a different simulation: instead of the FULL simulation use of the FLAT simulation**, i.e. p,d,t produced within the target with a FLAT Ekin spectrum in the range [5 MeV/u - 1 GeV/u] ( $\text{sys}_{\text{EpsDet}}$ )
- 4) **Unfolding procedure:** changing unfolding technique (RooUnfoldIDS) wrt the nominal one (RooUnfoldBayes) and compute the XSec difference ( $\text{sys}_{\text{unf}}$ )
- 5) **N<sup>12</sup>C from CNAO DDS:** 4% relative error from dose-current conversion uncertainty ( $\text{sys}_{\text{N12C}}$ )

# Final Results and MC comparison



Protons detected at 90°  
Production XSection from  
12C on PMMA target

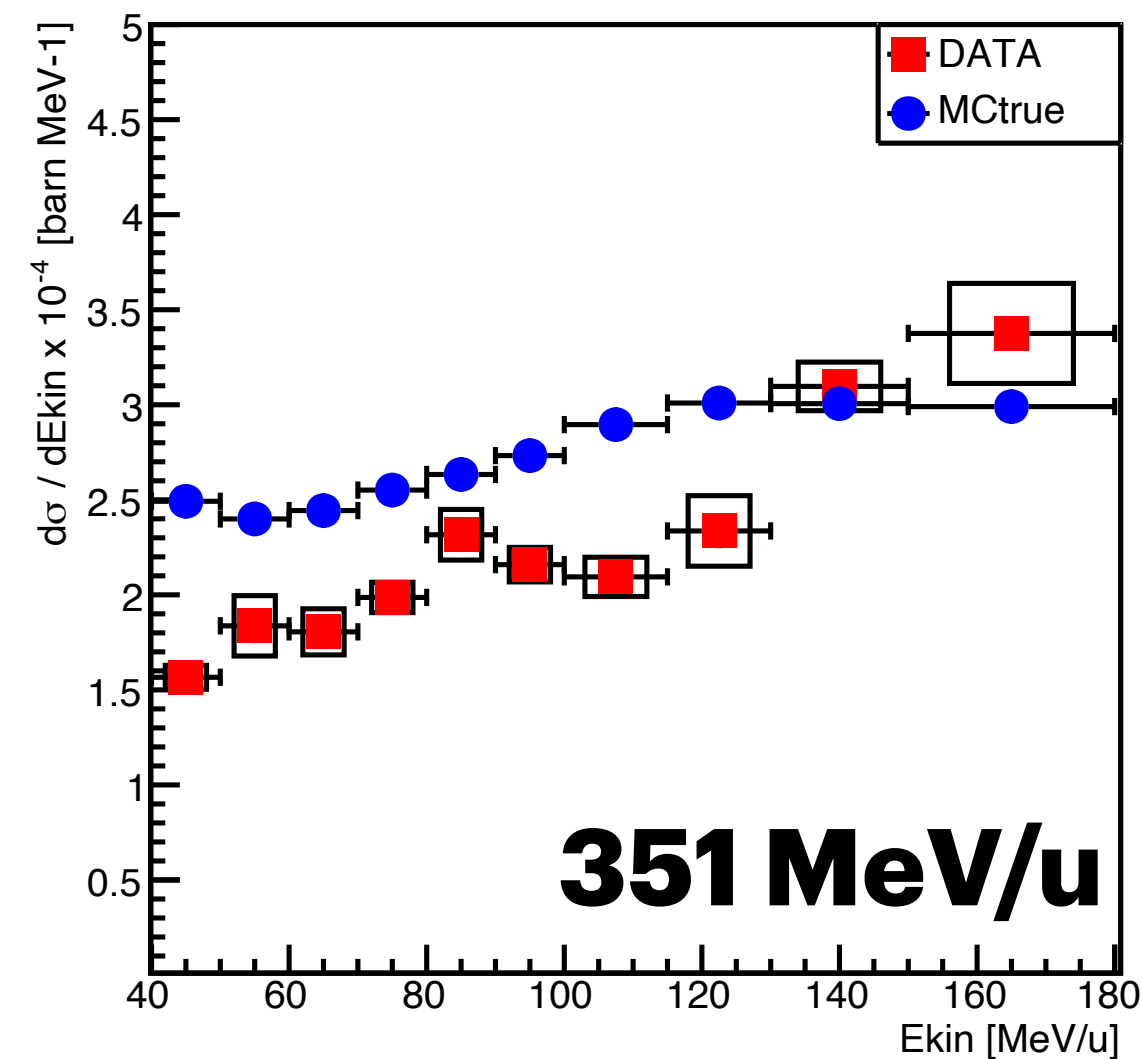
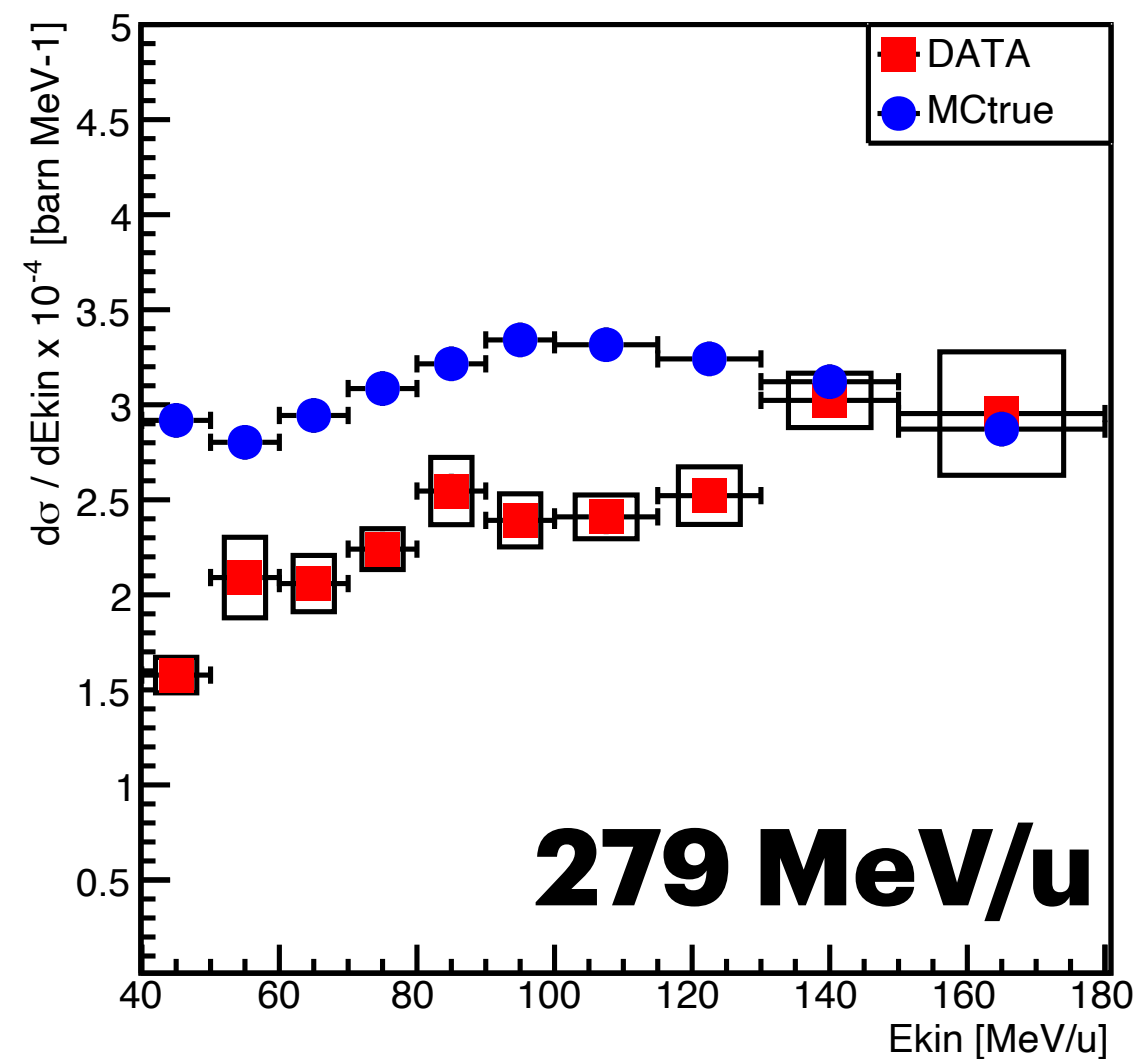
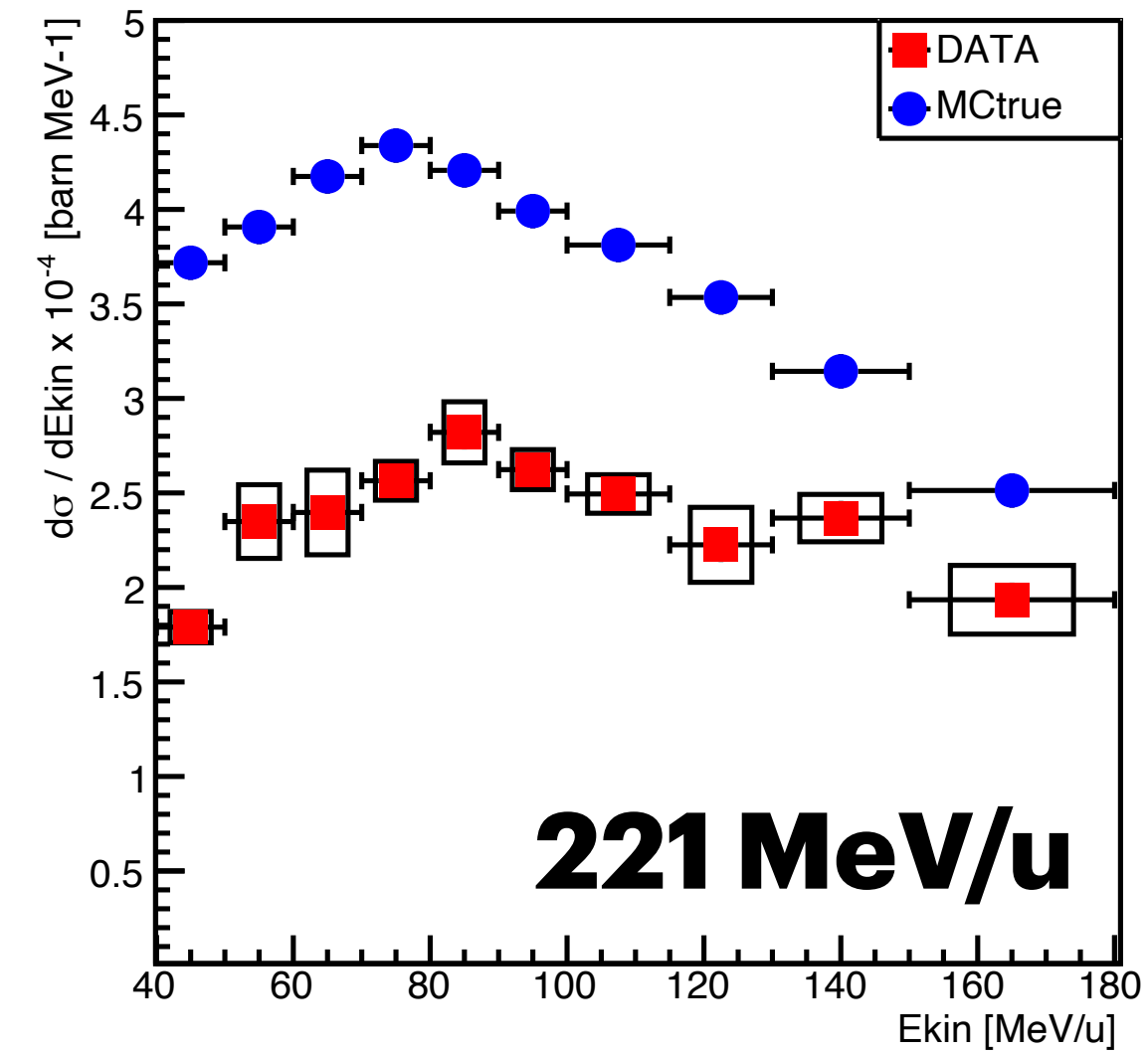
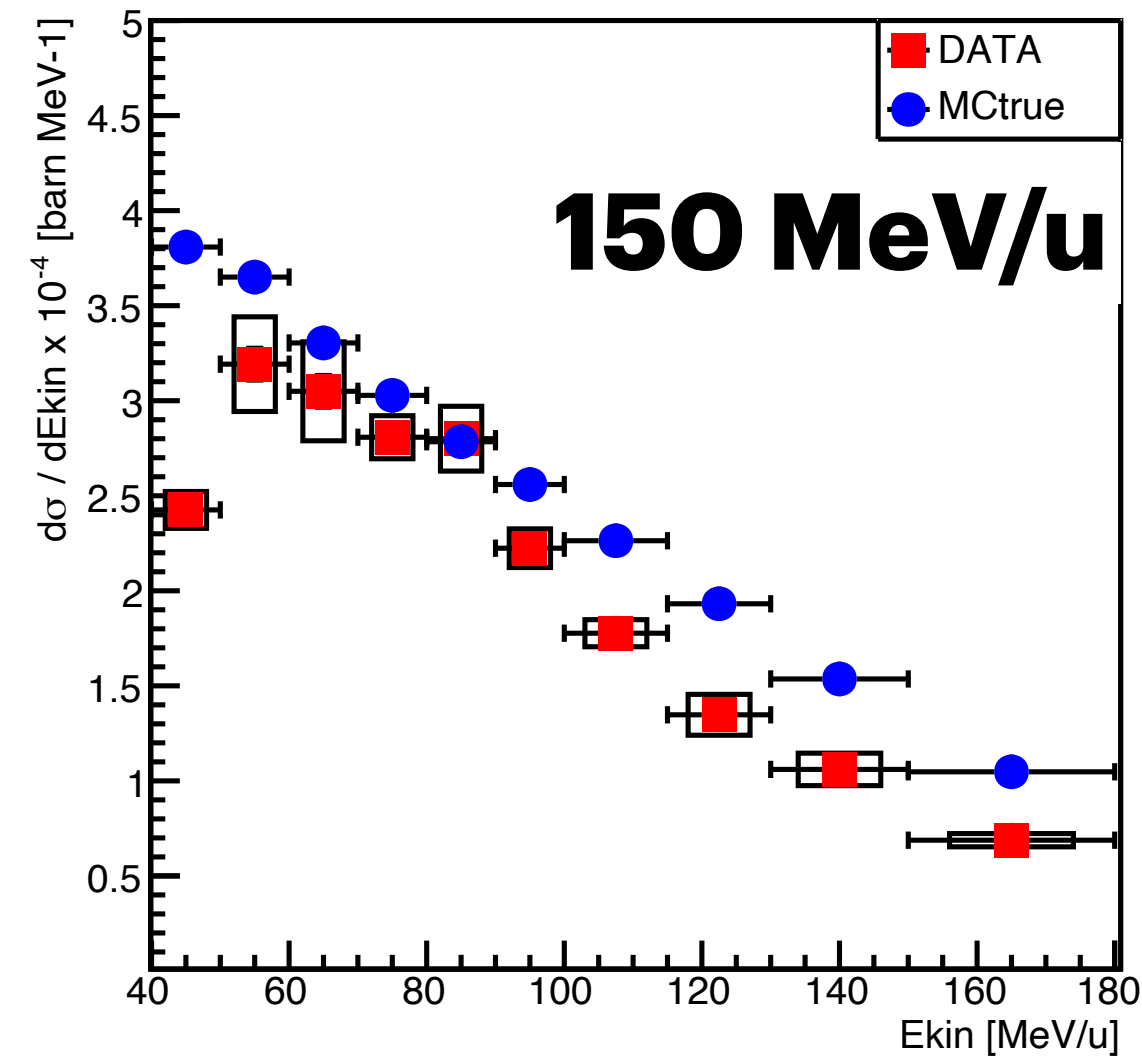
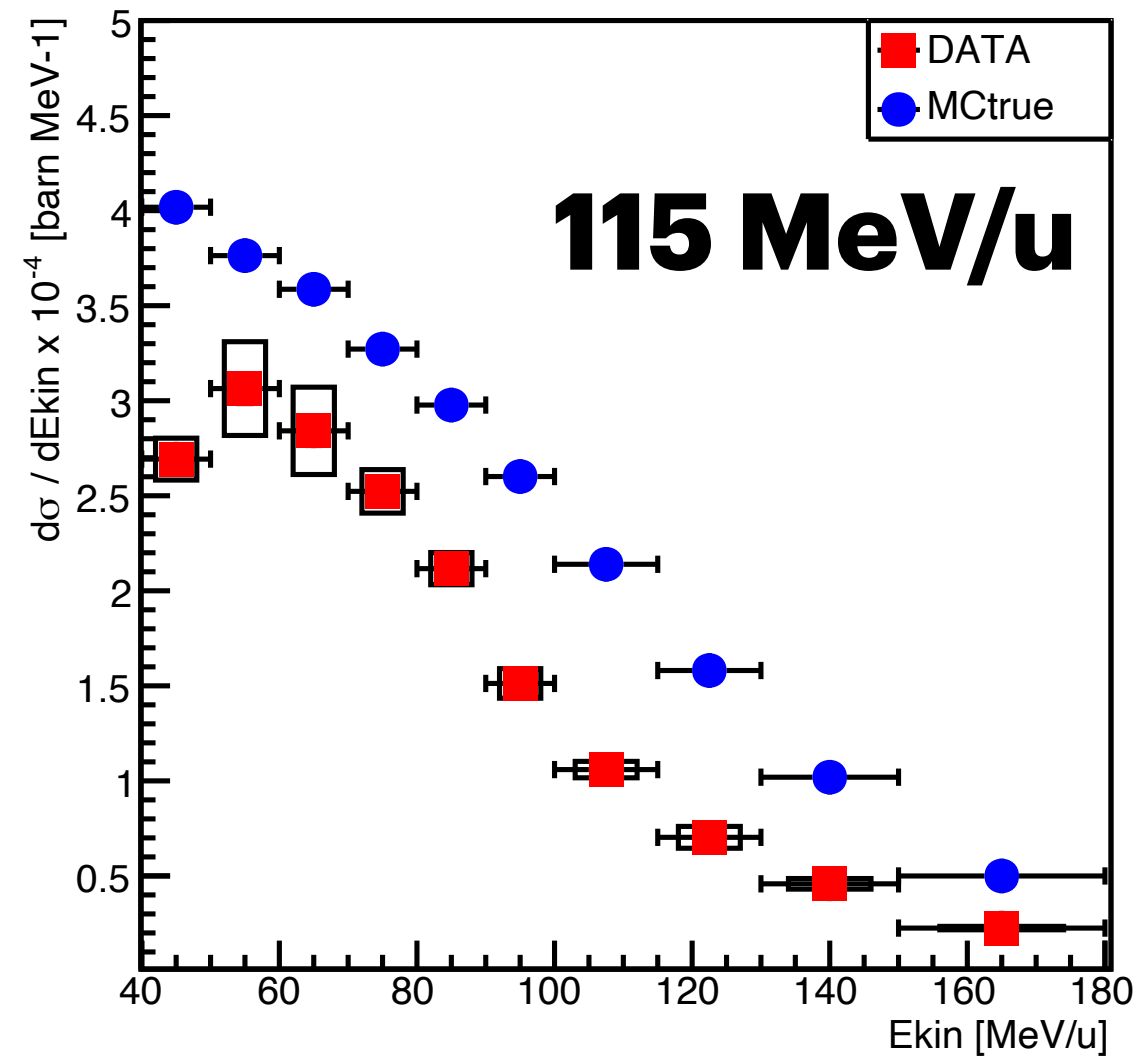
# Final Results and MC comparison



Protons detected at 60°  
Production XSection from  
12C on PMMA target

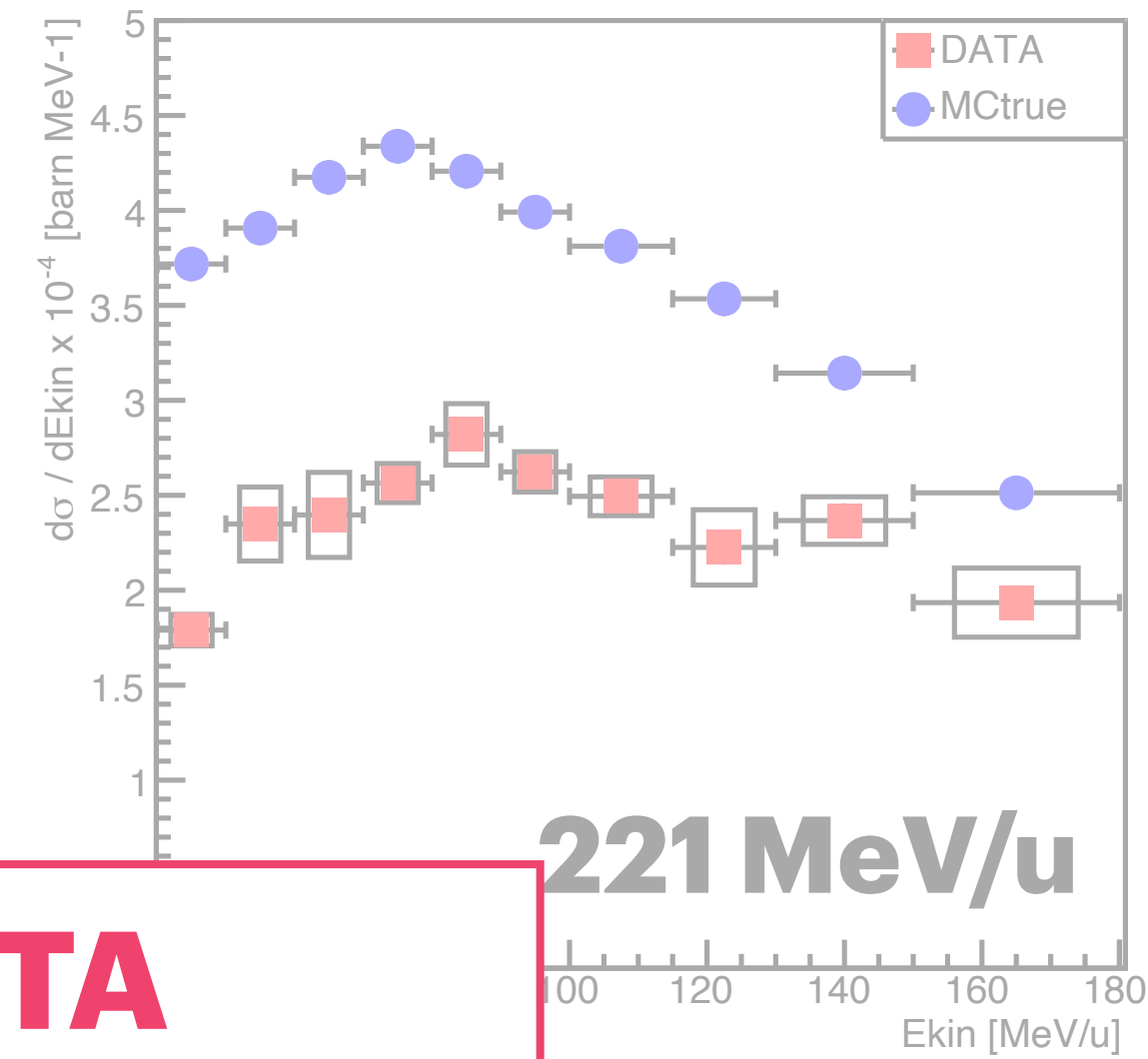
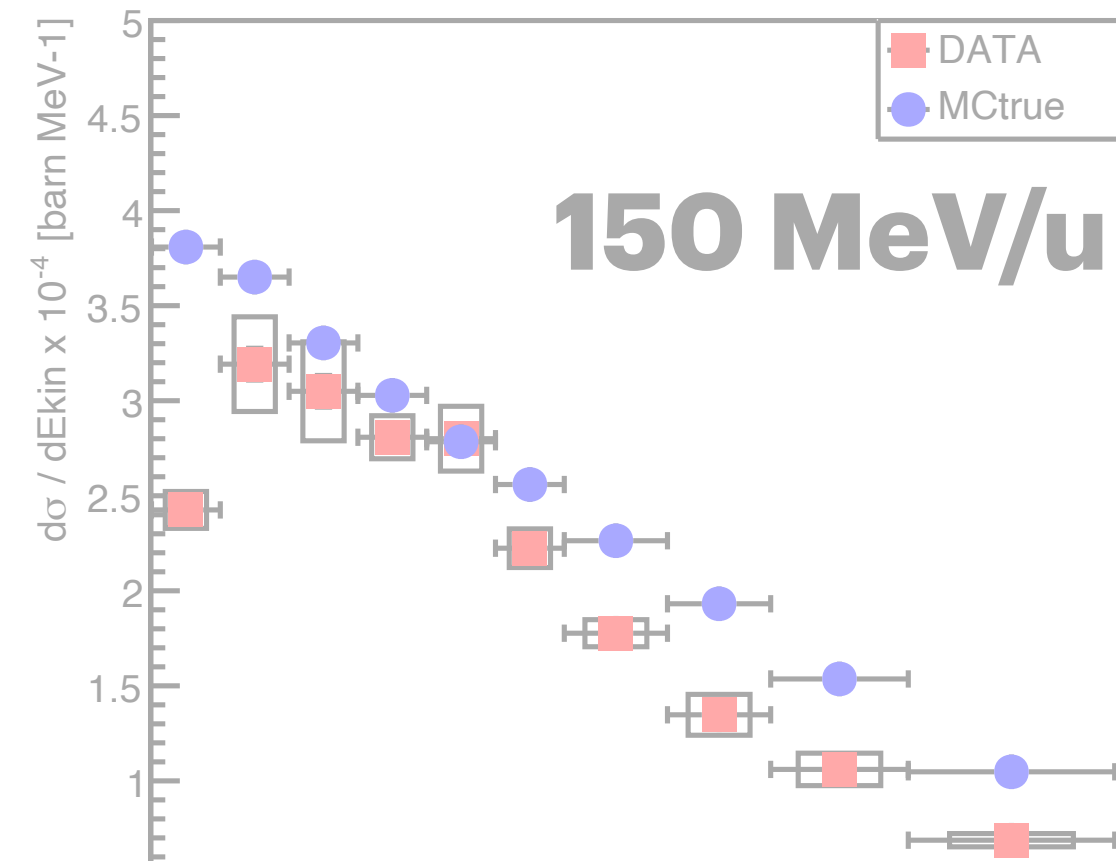
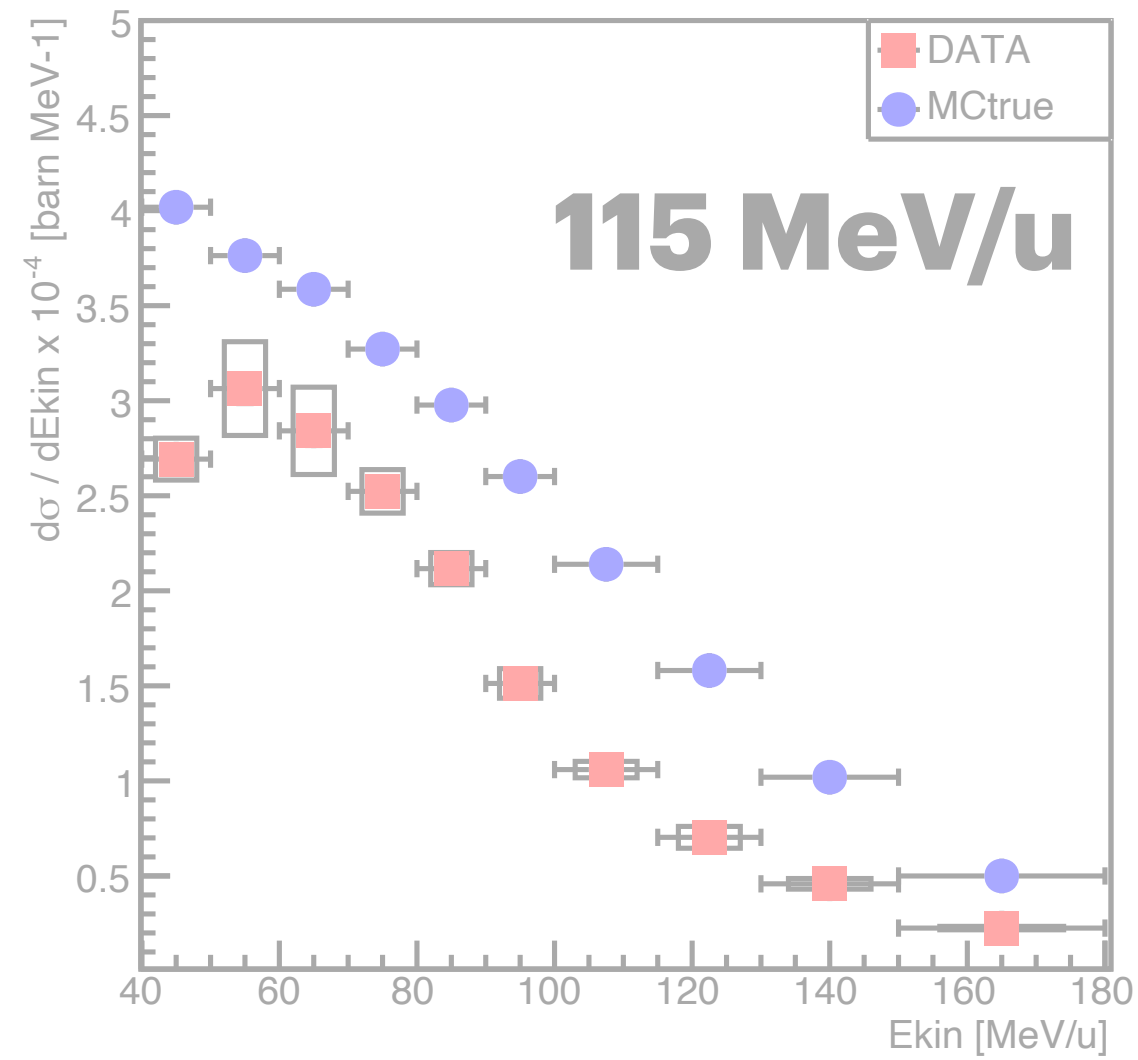


# Final Results and MC comparison

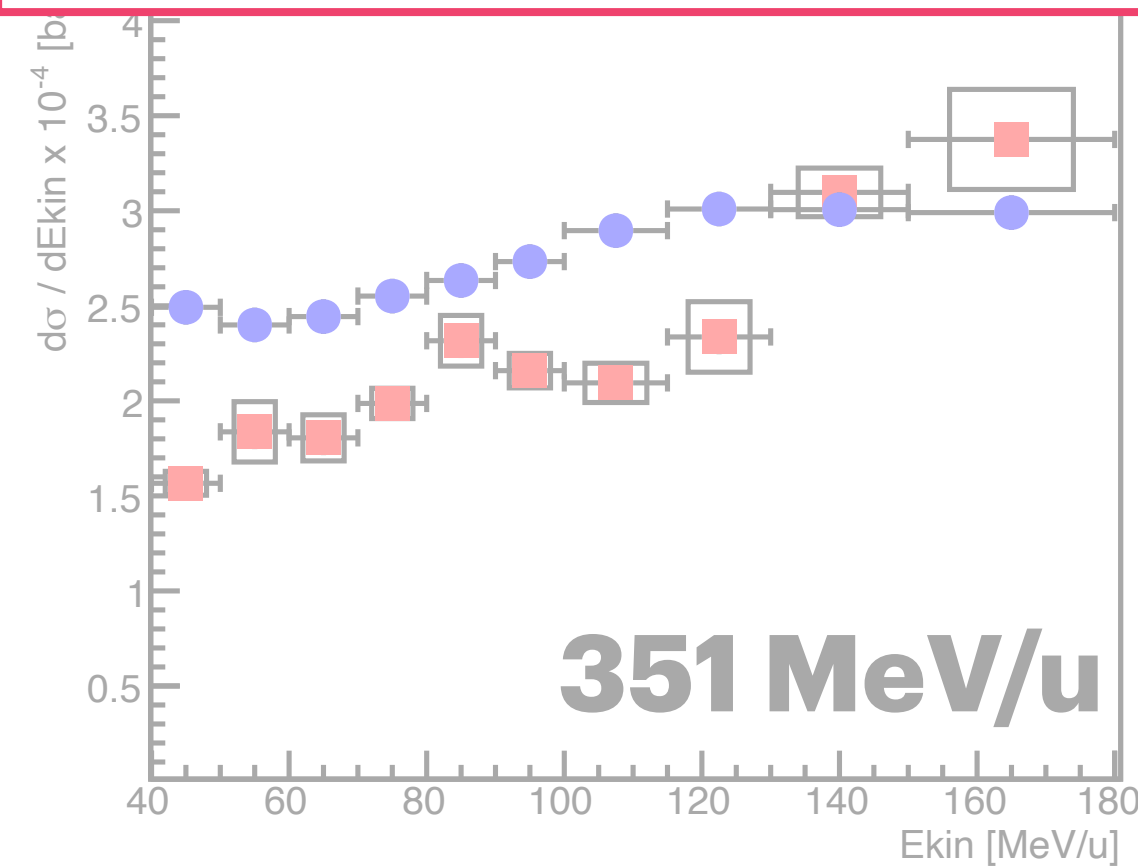
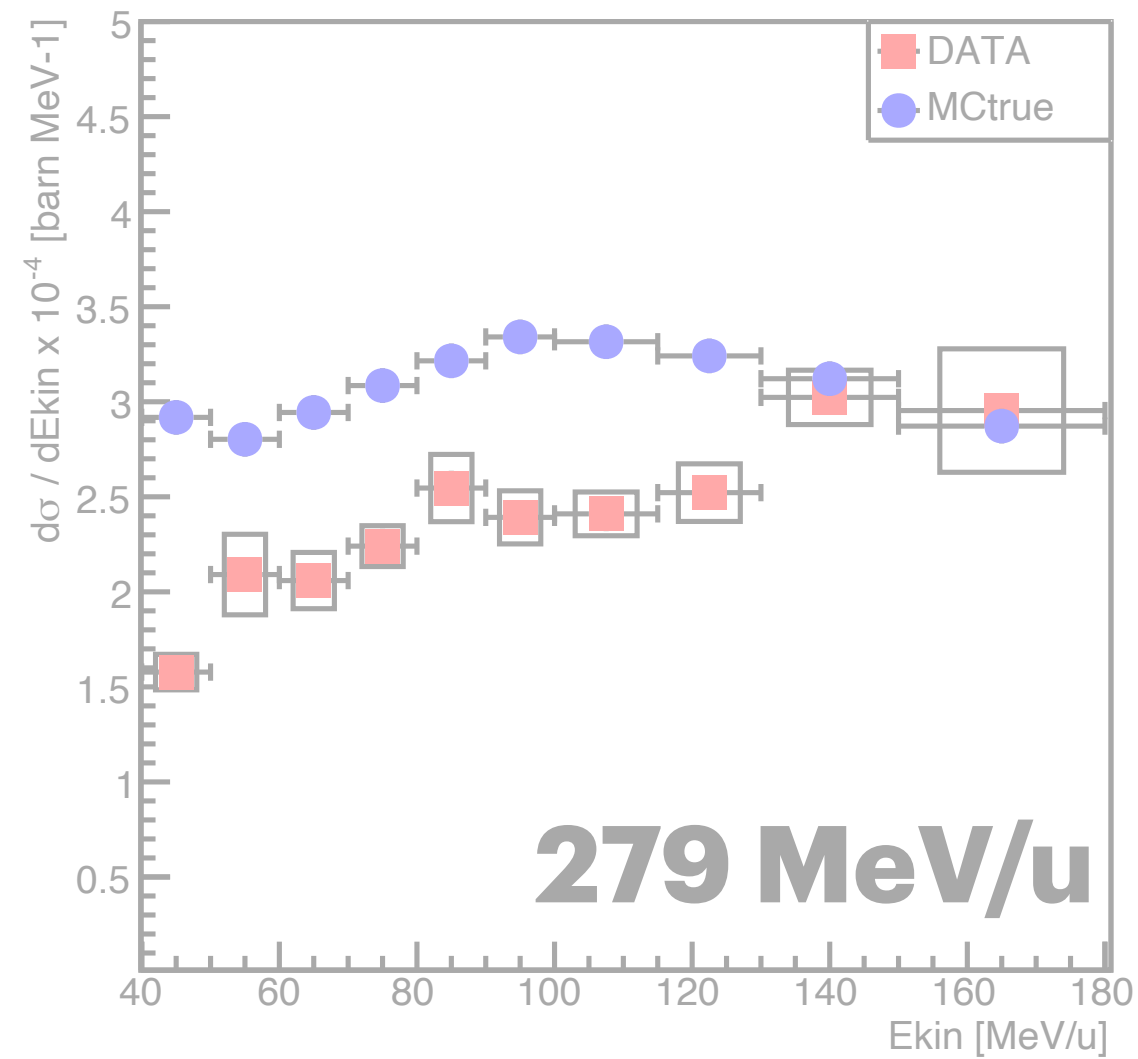


Protons detected at 32°  
Production XSection from  
12C on PMMA target

# Final Results and MC comparison

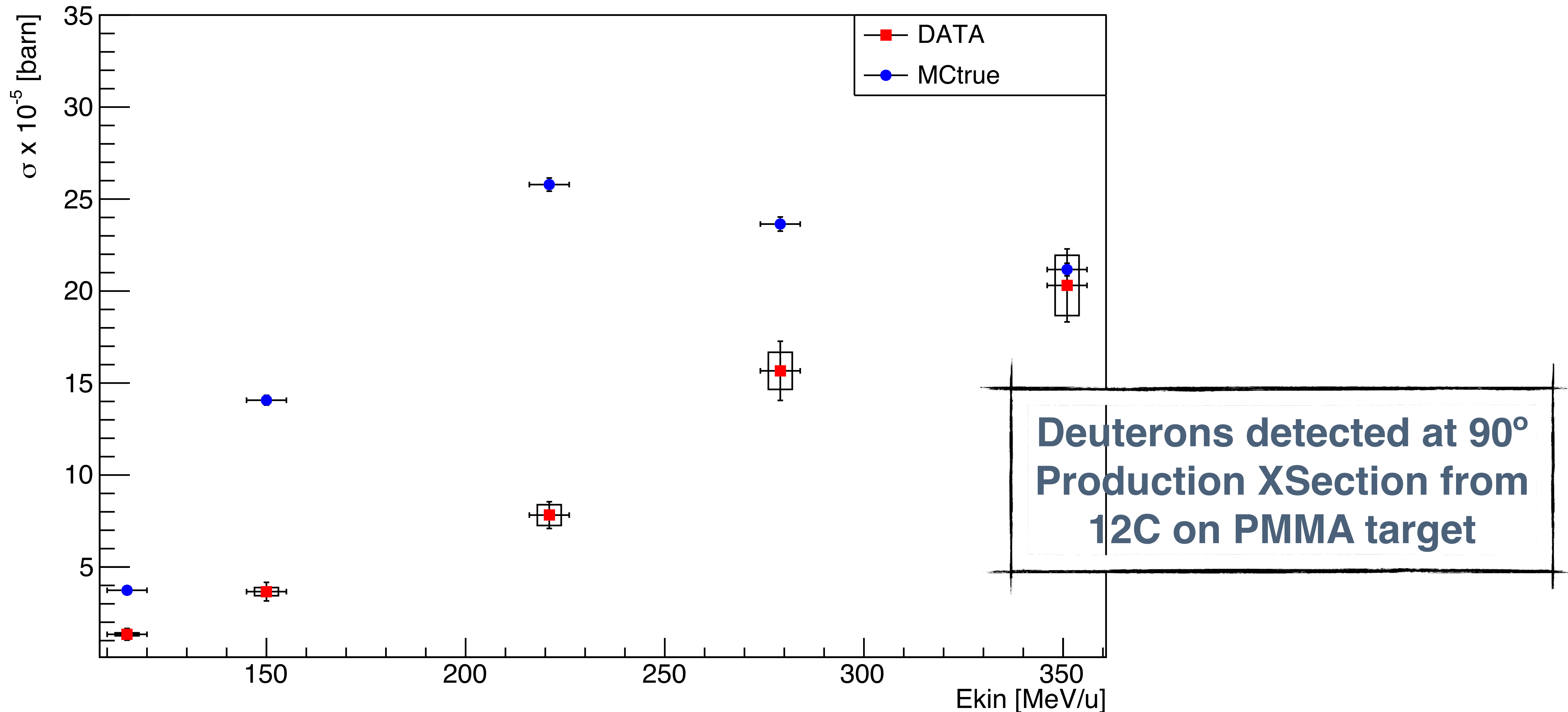


**Checks on DATA  
normalization (N<sup>12</sup>C, effDT)  
are ongoing.**

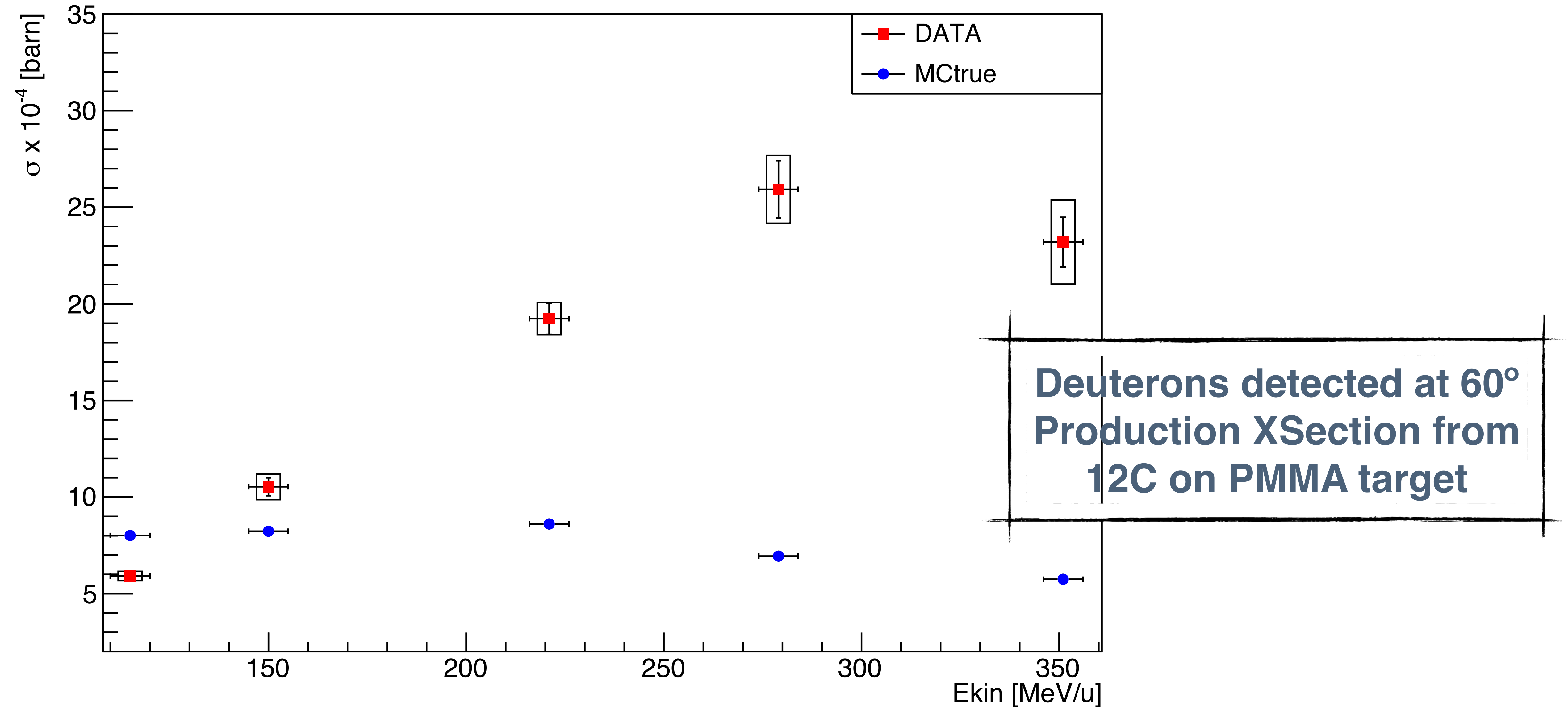


Protons detected at 32°  
Production XSection from  
12C on PMMA target

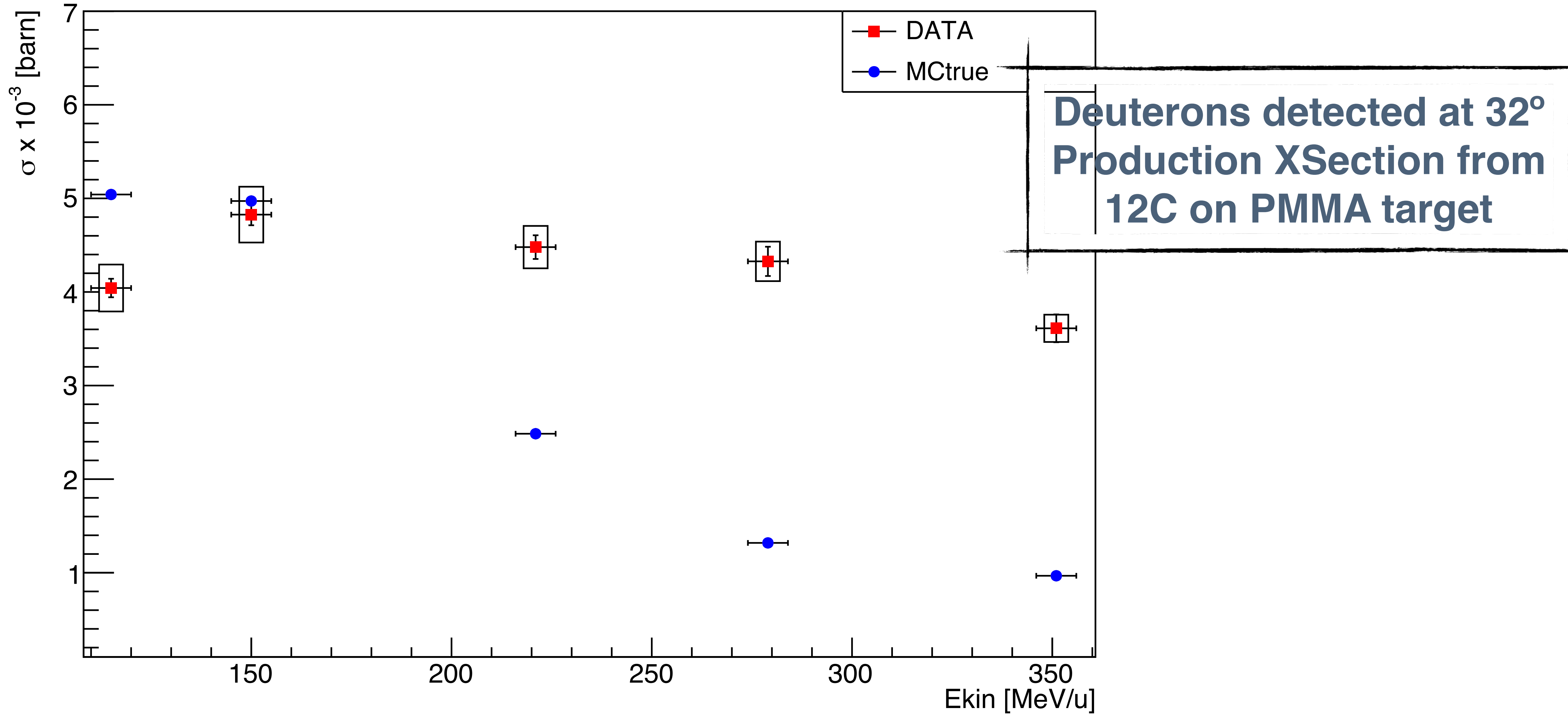
# Final Results and MC comparison



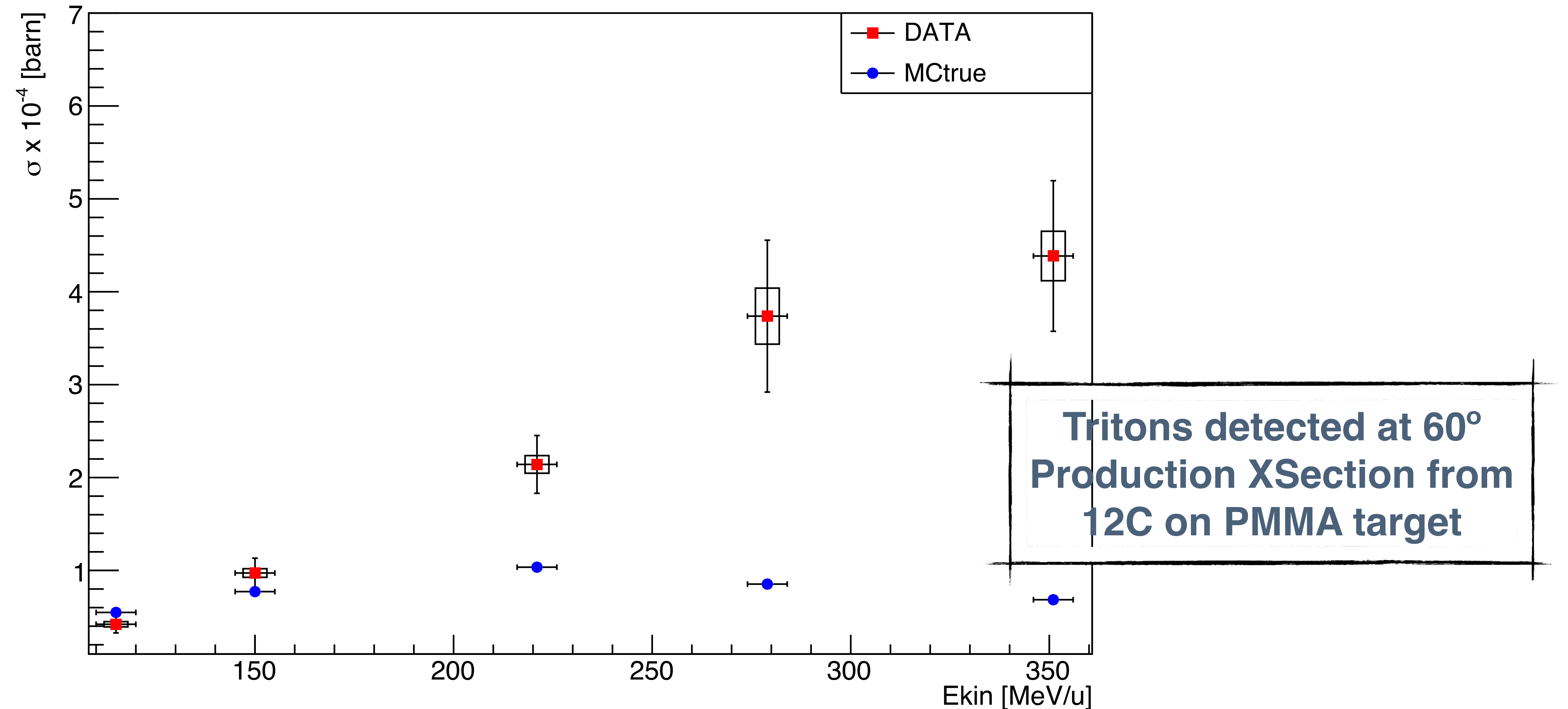
# Final Results and MC comparison



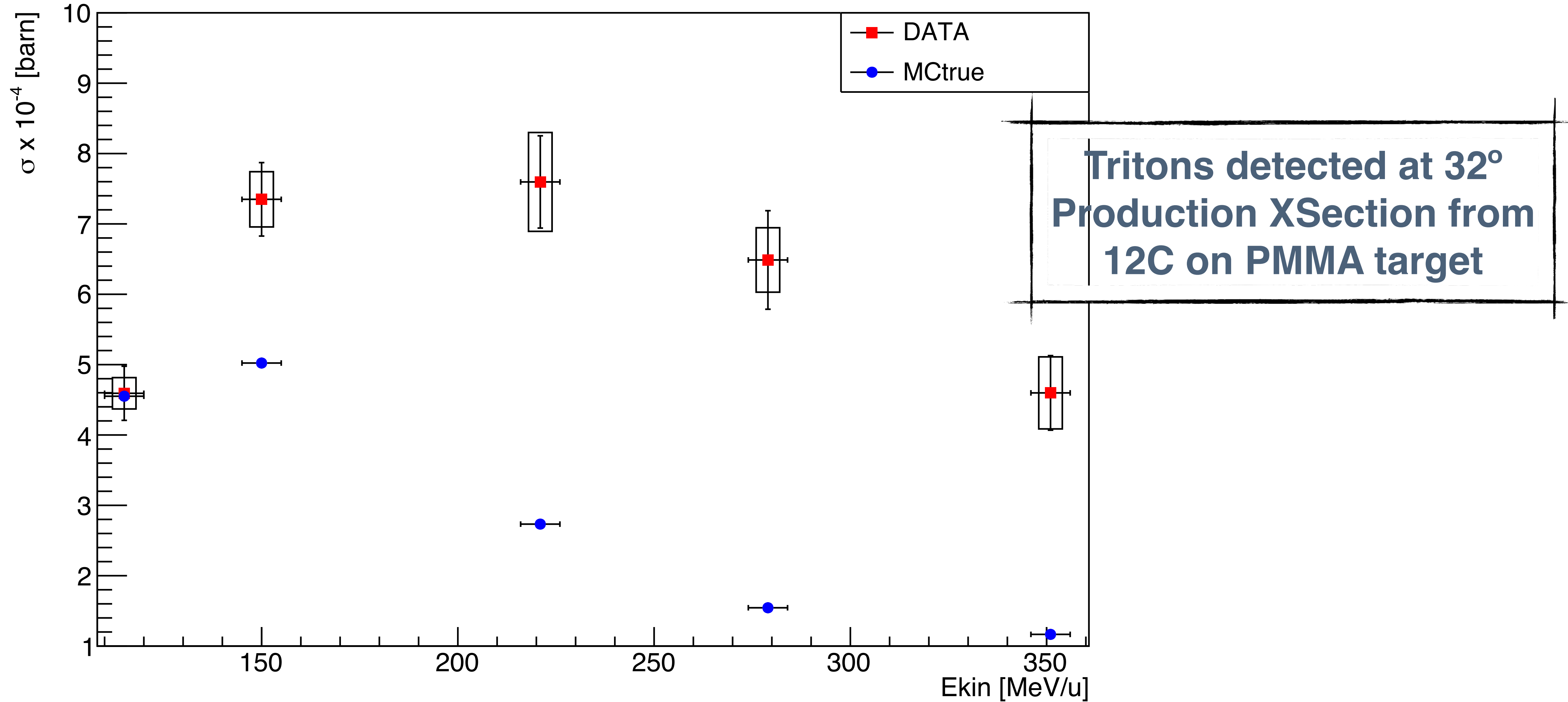
# Final Results and MC comparison



# Final Results and MC comparison



# Final Results and MC comparison



# Comparison with 2020 published results

To compare with old data published in 2020, the XSections have to be normalized to the LYSO  $\Delta\Omega$  ( $\Theta\pm 4^\circ$ ,  $\varphi\pm 4^\circ$  ( $6^\circ$ @ $32^\circ$ ))\*:

$$\frac{d\sigma^{\text{NEW}}}{dE_k} \left( \frac{A}{Z} X \right) = \frac{N_{\frac{A}{Z} X}(E_k)}{\Delta E_k} \cdot \frac{\text{purity}(E_k)}{N_{12C} N_Y} \cdot \frac{1}{\epsilon} \cdot \frac{1}{\Delta\Omega}$$

$$\frac{d\sigma^{\text{OLD}}}{dE_k} \left( \frac{A}{Z} X \right) = \frac{N_{\frac{A}{Z} X}(E_k)}{\Delta E_k} \cdot \frac{1}{N_{12C} N_Y} \cdot \frac{1}{\epsilon} \cdot \frac{1}{4\pi}$$

[\*the LYSO theoretical solid angle is  $\Theta, \varphi \pm 0.8^\circ$ ]



# Comparison with 2020 published results

PROTON PRODUCTION DIFFERENTIAL CROSS SECTION IN THE DIFFERENT ELEMENTS FROM CARBON ION BEAM ENERGY OF 221 MeV/u.

$E_{bin}^p$ [MeV]	$\delta_E$ [MeV]	$d\sigma_C^p/dE_k$ [b/sr/MeV]	p C 221								
$90^\circ$		$\cdot 10^{-4}$	$E_{kin}^p$ [MeV/u]	$\frac{d\sigma_{true}^{MC}}{dE_k}$	stat <sup>MC</sup> <sub>reco</sub>	sys <sup>PID</sup>	sys <sup>MC</sup> <sub>reco</sub>	sys <sup>MC</sup> <sub>unf</sub>	$\frac{d\sigma^{data}}{dE_k}$	stat <sup>data</sup>	sys <sup>data</sup>
			$90^\circ$	$\cdot 10^{-5}$ [b/sr]	[%]	[%]	[%]	[%]	$\cdot 10^{-5}$ [b/sr]	[%]	[%]
30-35	0	8.6 ± 1.3	40 - 60	32.7 ± 0.4	8.4	0.4	18.4	4.7	36.3 ± 2.2 ± 2.2	6.2	6.2
35-40	2	5.2 ± 0.6	60 - 80	16.5 ± 0.3	12.4	0.4	17.4	7.2	21.2 ± 1.9 ± 1.8	8.9	8.3
40-60	2	3.5 ± 0.2	80 - 100	8.1 ± 0.2	17.7	0.4	19.7	10.0	11.9 ± 1.6 ± 1.3	13.6	10.8
60-80	4	1.6 ± 0.1	100 - 120	4.0 ± 0.1	24.1	0.4	0.0	12.0	4.6 ± 0.8 ± 0.6	17.8	12.6
80-100	6	0.9 ± 0.1	120 - 140	2.2 ± 0.1	-0	0.4	-	-	2.1 ± 0.5 ± 0.3	23.8	12.6
100-120	10	0.4 ± 0.1	140 - 180	0.8 ± 0.0	-0	0.4	-	-	1.0 ± 0.3 ± 0.1	32.6	12.6
120-140	14	0.2 ± 0.1	180 - 250	0.2 ± 0.0	-0	0.4	-	-	-	-0	-
140-180	18	0.1 ± 0.1	250 - 350	-	-0	0.4	-	-	-	-0	-
			350 - 550	-	-0	0.4	-	-	-	-0	-
			550 - 750	-	-0	0.4	-	-	-	-0	-
			$60^\circ$	$\cdot 10^{-5}$ [b/sr]	[%]	[%]	[%]	[%]	$\cdot 10^{-5}$ [b/sr]	[%]	[%]
30-35	2	24.4 ± 3.4	40 - 60	129.3 ± 0.8	4.1	1.1	9.1	5.6	110.6 ± 3.5 ± 7.6	3.2	6.9
35-40	2	18.4 ± 2.0	60 - 80	95.4 ± 0.7	4.9	1.1	8.2	3.1	108.8 ± 4.0 ± 5.5	3.7	5.0
40-60	2	14.4 ± 0.8	80 - 100	67.2 ± 0.5	6.0	1.1	12.2	3.6	81.1 ± 3.5 ± 4.4	4.3	5.4
60-80	3	10.0 ± 0.6	100 - 120	42.7 ± 0.4	7.8	1.1	8.1	1.4	59.4 ± 3.3 ± 2.5	5.6	4.2
80-100	5	6.3 ± 0.4	120 - 140	24.1 ± 0.3	11.3	1.1	22.2	8.3	44.8 ± 3.4 ± 4.1	7.7	9.2
100-120	8	3.9 ± 0.2	140 - 160	13.2 ± 0.2	14.5	1.1	7.1	0.3	34.9 ± 3.7 ± 1.4	10.5	4.0
120-140	10	2.2 ± 0.1	160 - 180	7.0 ± 0.2	21.0	1.1	14.3	11.1	25.2 ± 3.9 ± 3.0	15.4	11.8
140-160	13	1.2 ± 0.1	180 - 200	4.1 ± 0.1	30.5	1.1	41.0	-	23.3 ± 5.5 ± 2.8	23.5	11.8
160-180	16	0.7 ± 0.1	200 - 230	1.9 ± 0.1	-0	1.1	-	-	18.0 ± 5.4 ± 2.1	30.0	11.8
180-200	20	0.4 ± 0.1	230 - 260	0.9 ± 0.1	-0	1.1	-	-	9.7 ± 4.3 ± 1.2	43.9	11.8
200-230	23	0.2 ± 0.1	260 - 290	0.5 ± 0.0	-0	1.1	-	-	2.7 ± 1.1 ± 0.3	41.2	11.8
230-260	27	0.1 ± 0.1	290 - 350	0.2 ± 0.0	-0	1.1	-	-	1.8 ± 1.1 ± 0.2	60.6	11.8
260-290	33	0.1 ± 0.1	350 - 450	0.0 ± 0.0	-0	1.1	-	-	-	-0	-
290-350	40	-	450 - 650	-	-0	1.1	-	-	-	-0	-
			650 - 850	-	-0	1.1	-	-	-	-0	-

90°	RATIO NEW/OLD
40-60	1.04
60-80	1.33
80-100	1.32
100-120	1.15
120-140	1.05
140-180	1.00
180-250	-

60°	RATIO NEW/OLD
40-60	0.77
60-80	1.09
80-100	1.29
100-120	1.52
120-140	2.04
140-160	2.91
160-180	3.60
180-200	5.83
200-230	9.00
230-260	9.70
260-290	2.70
290-350	-

# Comparison with 2020 published results

$E_{kin}^C$ [MeV/u]	$\sigma_C^p$ [barn /sr]	$\sigma_O^p$ [barn /sr]	$\sigma_H^p$ [barn /sr]
90°	$\cdot 10^{-3}$	$\cdot 10^{-3}$	$\cdot 10^{-5}$
115	8.97 ± 0.63	12.77 ± 2.48	11.44 ± 7.88
153	12.45 ± 0.89	19.52 ± 3.29	6.25 ± 9.43
221	18.87 ± 1.22	27.43 ± 4.48	16.28 ± 19.08
281	23.58 ± 1.50	33.17 ± 5.24	6.78 ± 19.62
353	28.23 ± 1.76	44.35 ± 6.08	25.05 ± 29.16
60°	$\cdot 10^{-2}$	$\cdot 10^{-2}$	$\cdot 10^{-2}$
115	5.84 ± 0.52	7.68 ± 1.06	0.50 ± 0.23
153	7.90 ± 0.74	9.90 ± 1.36	0.69 ± 0.29
221	10.99 ± 1.02	15.12 ± 1.90	1.10 ± 0.37
281	12.92 ± 1.19	18.10 ± 2.19	1.38 ± 0.40
353	14.75 ± 1.36	21.36 ± 2.48	1.38 ± 0.44

90°	RATIO NEW/OLD bin sum	RATIO NEW/OLD 1 bin
115	0.62	0.67
153	0.77	0.78
221	0.83	0.83
281	0.84	0.79
353	0.85	0.83

60°	RATIO NEW/OLD bin sum	RATIO NEW/OLD 1 bin
115	0.89	0.86
153	0.86	0.82
221	0.98	0.90
281	0.99	0.90
353	1.08	0.95

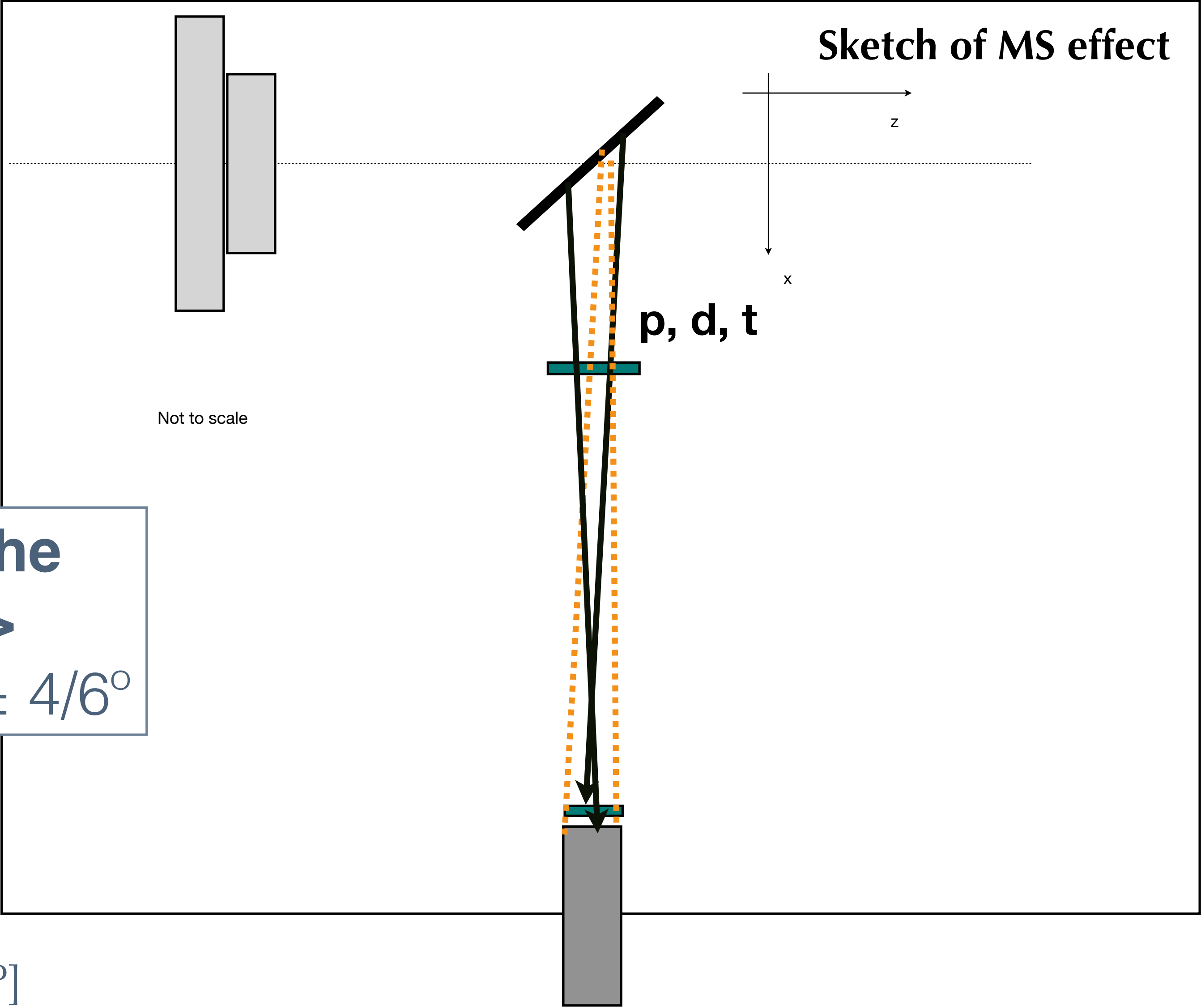
**p C 1 bin - eff ave**

$E_{kin}^C$ [MeV/u]	$\sigma_{true}^{MC}$	stat $_{reco}^{MC}$	sys $_{PID}$	sys $_{reco}^{MC}$	sys $_{un.f}^{MC}$	$\sigma^{data}$	stat $^{data}$	sys $^{data}$
90°	$\cdot 10^{-3}$ [b/sr]	[%]	[%]	[%]	[%]	$\cdot 10^{-3}$ [b/sr]	[%]	[%]
115	6.3 ± 0.1	8.3	0.3	7.1	3.4	6.0 ± 0.4 ± 0.3	6.3	5.3
150	9.0 ± 0.1	7.2	0.4	6.4	3.1	9.7 ± 0.5 ± 0.5	5.4	5.1
221	13.1 ± 0.1	6.0	0.4	8.3	1.3	15.6 ± 0.7 ± 0.7	4.5	4.2
279	16.3 ± 0.1	5.1	0.5	5.8	3.5	18.7 ± 0.7 ± 1.0	3.9	5.3
351	20.1 ± 0.1	4.7	0.6	6.4	2.0	23.5 ± 0.8 ± 1.1	3.5	4.5
60°	$\cdot 10^{-2}$ [b/sr]	[%]	[%]	[%]	[%]	$\cdot 10^{-2}$ [b/sr]	[%]	[%]
115	4.2 ± 0.0	3.4	0.6	13.2	0.5	5.0 ± 0.1 ± 0.2	2.5	4.0
150	4.0 ± 0.0	3.4	0.8	10.3	1.2	6.5 ± 0.2 ± 0.3	2.4	4.2
221	7.8 ± 0.0	2.5	1.1	8.5	2.5	9.9 ± 0.2 ± 0.5	1.8	4.7
279	10.6 ± 0.0	2.1	1.3	7.6	1.7	11.6 ± 0.2 ± 0.5	1.6	4.4
351	12.9 ± 0.0	2.0	1.5	5.3	2.0	14.0 ± 0.2 ± 0.6	1.5	4.5

Bin sum $\sigma^{data}$	stat $^{data}$	sys $^{data}$
$\cdot 10^{-3}$ [b/sr]	[%]	[%]
5.6 ± 0.4 ± 0.3	6.5	5.3
9.6 ± 0.5 ± 0.5	5.6	5.1
15.6 ± 0.7 ± 0.7	4.5	4.2
19.9 ± 1.0 ± 1.1	5.0	5.3
24.0 ± 0.9 ± 1.1	3.7	4.5
$\cdot 10^{-2}$ [b/sr]	[%]	[%]
5.2 ± 0.2 ± 0.2	4.2	4.0
6.8 ± 0.3 ± 0.3	3.9	4.2
10.8 ± 0.3 ± 0.5	2.9	4.7
12.8 ± 0.4 ± 0.6	2.8	4.4
15.9 ± 0.4 ± 0.7	2.3	4.5

# Comparison with 2020 published results

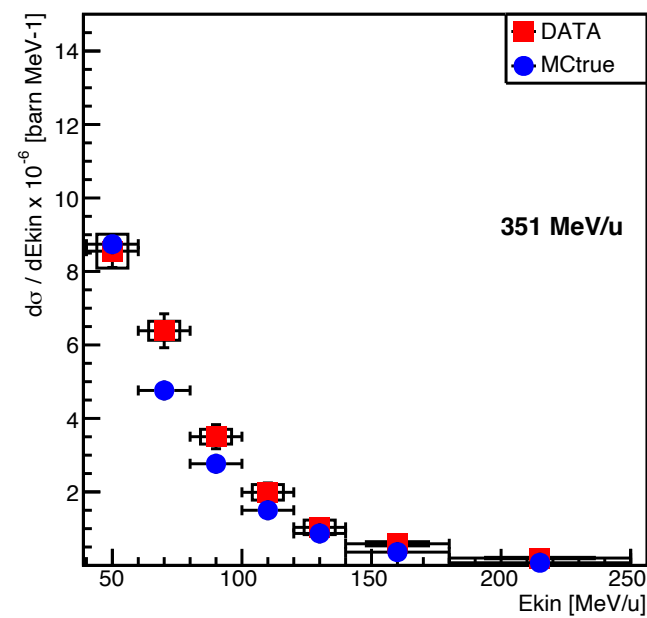
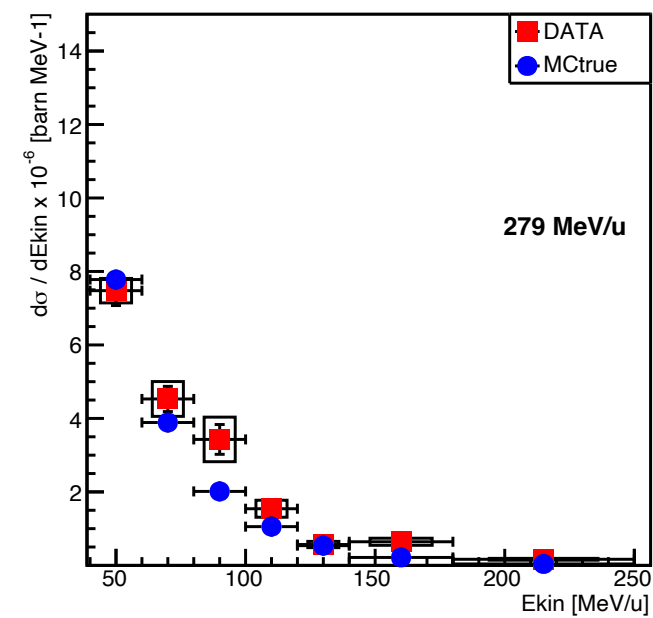
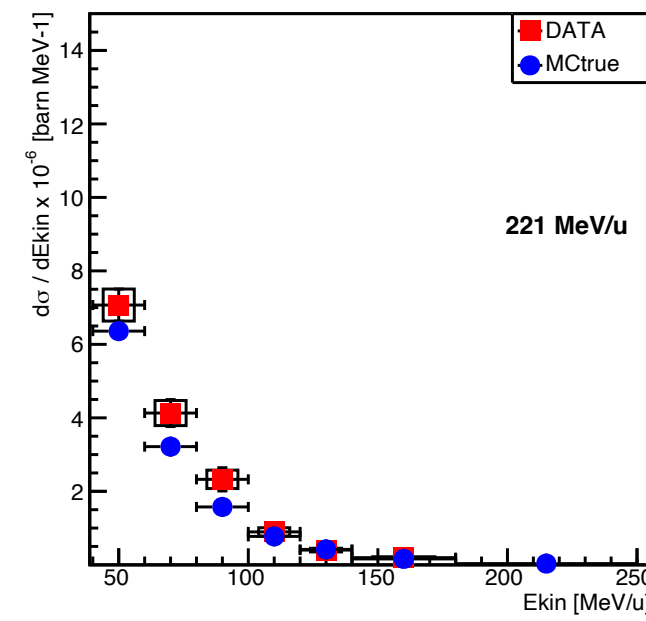
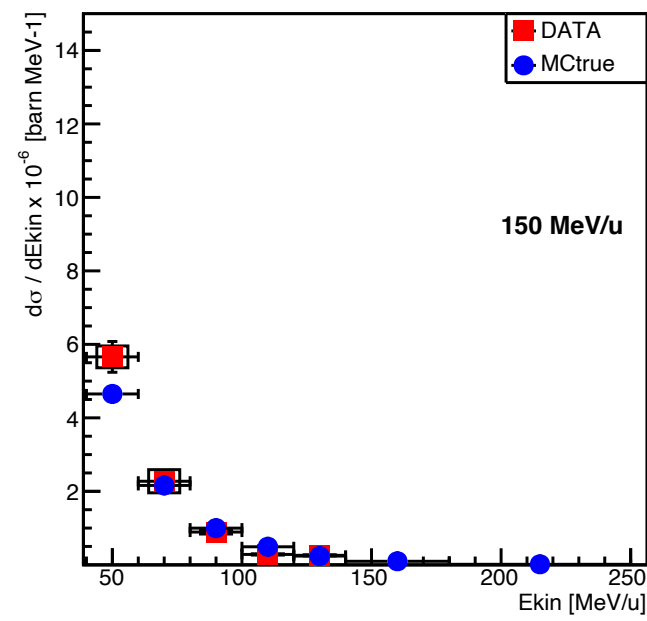
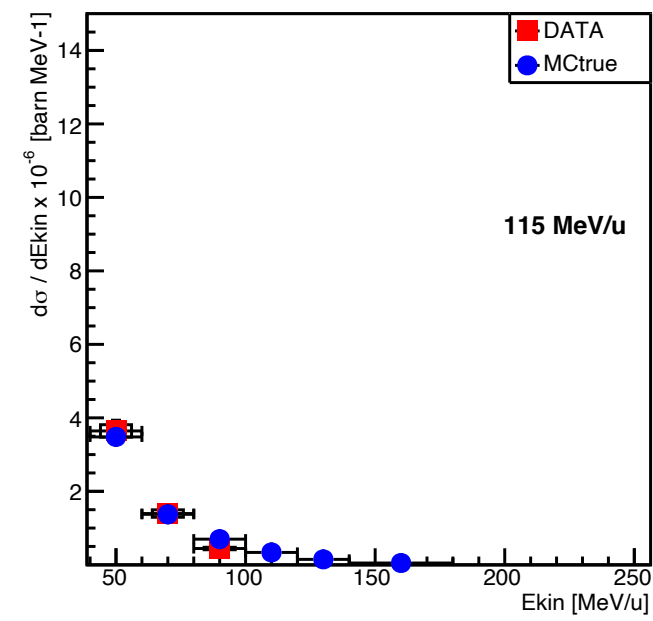
The **remaining difference** between the **old published analysis** and the **new analysis** is due to the **Multiple Scattering** that has been taken into account in the detection efficiency of new analysis and has NOT in the old analysis



[\*the LYSO theoretical solid angle is  $\Theta, \varphi \pm 0.8^\circ$ ]

# Conclusions

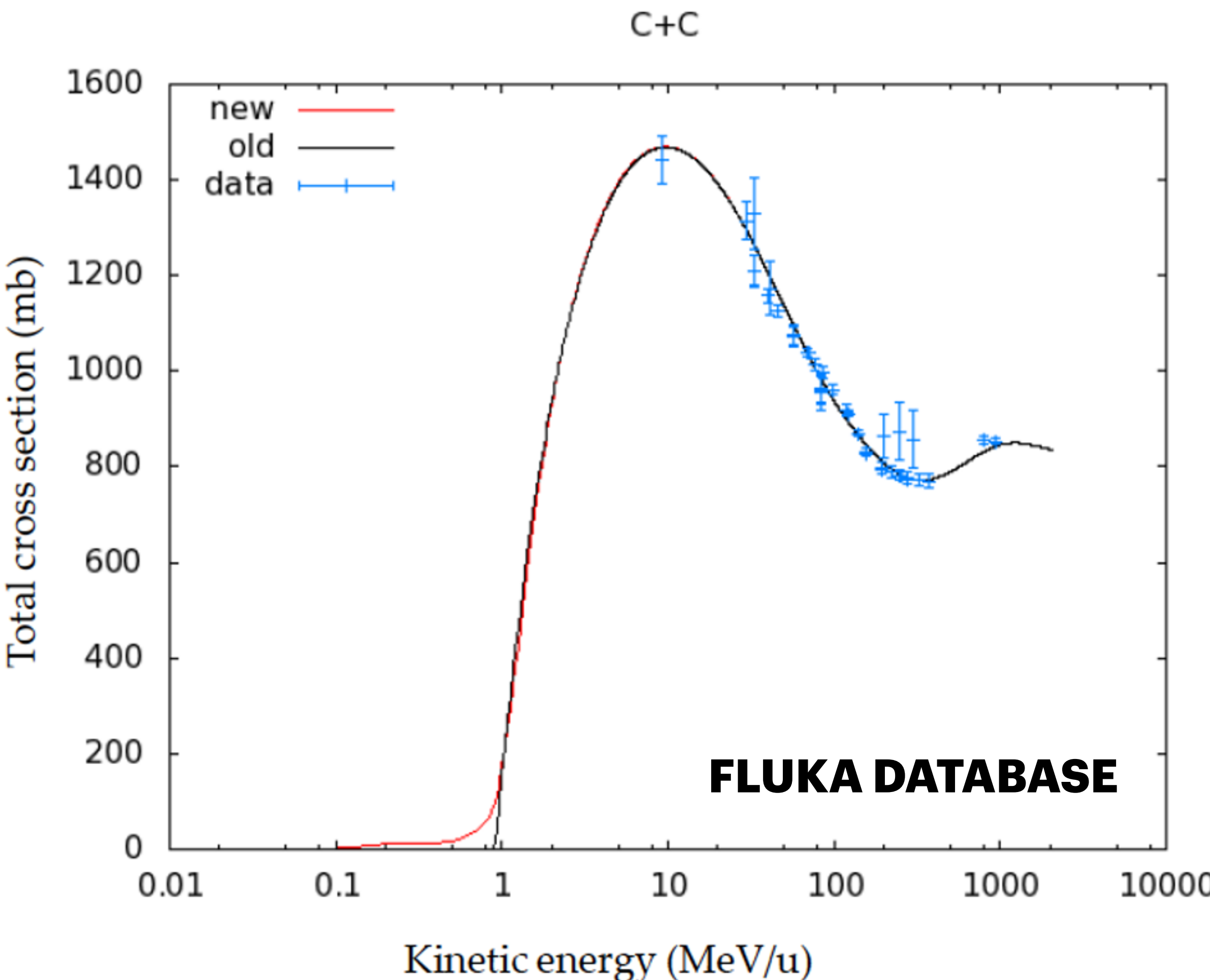
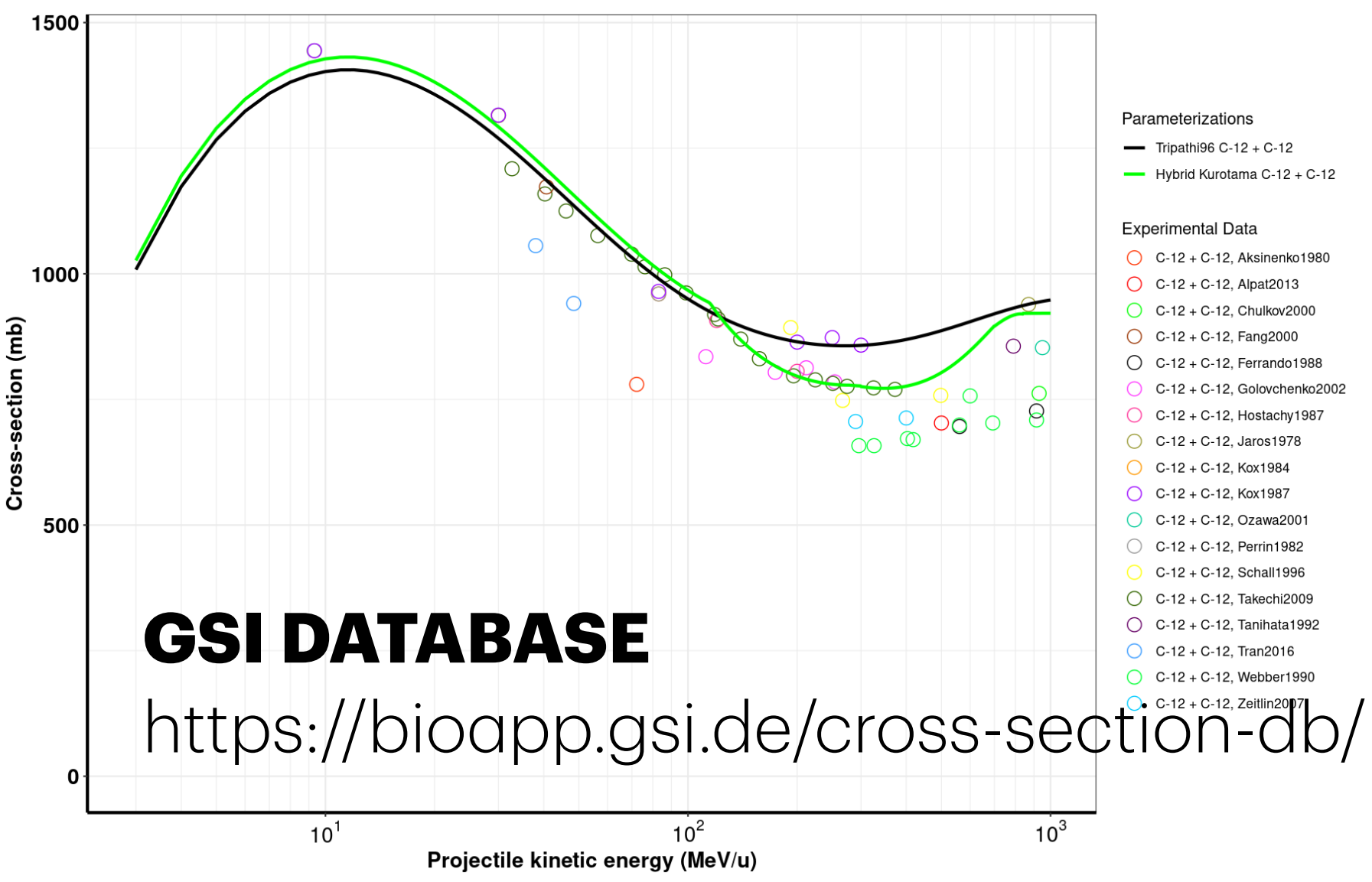
- Small effort more to assess the 32deg analysis normalization
- The systematic errors from detection efficiency and PID selection have to be added to the total systematic error



p C 115								
$E_{kin}^p$ [MeV/u]	$\frac{d\sigma_{true}^{MC}}{dE_k}$	$stat_{reco}^{MC}$	$sys_{PID}$	$sys_{reco}^{MC}$	$sys_{unf}^{MC}$	$\frac{d\sigma^{data}}{dE_k}$	$stat^{data}$	$sys^{data}$
90°	$\cdot 10^{-6}$ [b]	[%]	[%]	[%]	[%]	$\cdot 10^{-6}$ [b]	[%]	[%]
40 - 60	$3.5 \pm 0.1$	11.1	0.5	20.9	2.4	$3.6 \pm 0.3 \pm 0.2$	8.0	4.6
60 - 80	$1.4 \pm 0.0$	17.1	0.5	0.0	6.0	$1.4 \pm 0.2 \pm 0.1$	13.1	7.3
80 - 100	$0.7 \pm 0.0$	26.1	0.5	7.1	6.4	$0.4 \pm 0.1 \pm 0.0$	20.4	7.6
100 - 120	$0.3 \pm 0.0$	-	0.5	-	-	-	-	-
120 - 140	$0.1 \pm 0.0$	-	0.5	-	-	-	-	-
140 - 180	$0.0 \pm 0.0$	-	0.5	-	-	-	-	-
180 - 250	-	-	0.5	-	-	-	-	-
250 - 350	-	-	0.5	-	-	-	-	-
350 - 550	-	-	0.5	-	-	-	-	-
550 - 750	-	-	0.5	-	-	-	-	-
60°	$\cdot 10^{-6}$ [b]	[%]	[%]	[%]	[%]	$\cdot 10^{-6}$ [b]	[%]	[%]
40 - 60	$15.1 \pm 0.1$	5.1	0.7	16.7	0.8	$15.7 \pm 0.6 \pm 0.6$	3.8	4.1
60 - 80	$10.0 \pm 0.1$	6.6	0.7	16.5	4.3	$12.0 \pm 0.6 \pm 0.7$	4.7	5.9
80 - 100	$5.3 \pm 0.1$	9.1	0.7	1.5	8.7	$7.0 \pm 0.5 \pm 0.7$	6.7	9.6
100 - 120	$2.4 \pm 0.0$	13.3	0.7	11.0	4.2	$3.5 \pm 0.3 \pm 0.2$	9.5	5.8
120 - 140	$1.2 \pm 0.0$	18.9	0.7	15.0	13.9	$1.7 \pm 0.2 \pm 0.2$	13.1	14.4
140 - 160	$0.6 \pm 0.0$	28.9	0.7	28.6	29.8	$1.4 \pm 0.3 \pm 0.4$	21.9	30.1
160 - 180	$0.3 \pm 0.0$	-	0.7	-	-	$0.5 \pm 0.1 \pm 0.2$	25.3	30.1
180 - 200	$0.2 \pm 0.0$	-	0.7	-	-	$0.3 \pm 0.1 \pm 0.1$	33.6	30.1
200 - 230	$0.1 \pm 0.0$	-	0.7	-	-	$1.0 \pm 1.0 \pm 0.3$	97.0	30.1
230 - 260	$0.0 \pm 0.0$	-	0.7	-	-	-	-	-
260 - 290	$0.0 \pm 0.0$	-	0.7	-	-	-	-	-
290 - 350	-	-	0.7	-	-	-	-	-
350 - 450	-	-	0.7	-	-	-	-	-
450 - 650	-	-	0.7	-	-	-	-	-
650 - 850	-	-	0.7	-	-	-	-	-
32°	$\cdot 10^{-6}$ [b]	[%]	[%]	[%]	[%]	$\cdot 10^{-6}$ [b]	[%]	[%]
40 - 50	$4.2 \pm 0.0$	4.1	1.3	10.8	0.5	$3.1 \pm 0.1 \pm 0.1$	3.8	4.0
50 - 60	$3.9 \pm 0.0$	4.2	1.3	2.0	7.4	$3.7 \pm 0.2 \pm 0.3$	4.1	8.4
60 - 70	$3.7 \pm 0.0$	4.2	1.3	6.7	4.7	$2.9 \pm 0.1 \pm 0.2$	4.2	6.2
70 - 80	$3.4 \pm 0.0$	4.6	1.3	4.8	5.8	$2.7 \pm 0.1 \pm 0.2$	4.5	7.0
80 - 90	$3.1 \pm 0.0$	4.9	1.3	5.4	0.9	$2.3 \pm 0.1 \pm 0.1$	4.6	4.1
90 - 100	$2.7 \pm 0.0$	5.2	1.3	10.9	7.4	$1.6 \pm 0.1 \pm 0.1$	4.9	8.4
100 - 115	$2.3 \pm 0.0$	4.9	1.3	8.0	0.9	$1.2 \pm 0.1 \pm 0.0$	5.1	4.1
115 - 130	$1.7 \pm 0.0$	5.8	1.3	12.1	8.0	$0.8 \pm 0.0 \pm 0.1$	5.7	8.9
130 - 150	$1.1 \pm 0.0$	6.2	1.3	7.1	3.4	$0.6 \pm 0.0 \pm 0.0$	6.3	5.2
150 - 180	$0.5 \pm 0.0$	7.7	1.3	3.0	2.6	$0.3 \pm 0.0 \pm 0.0$	8.8	4.8

# Conclusions

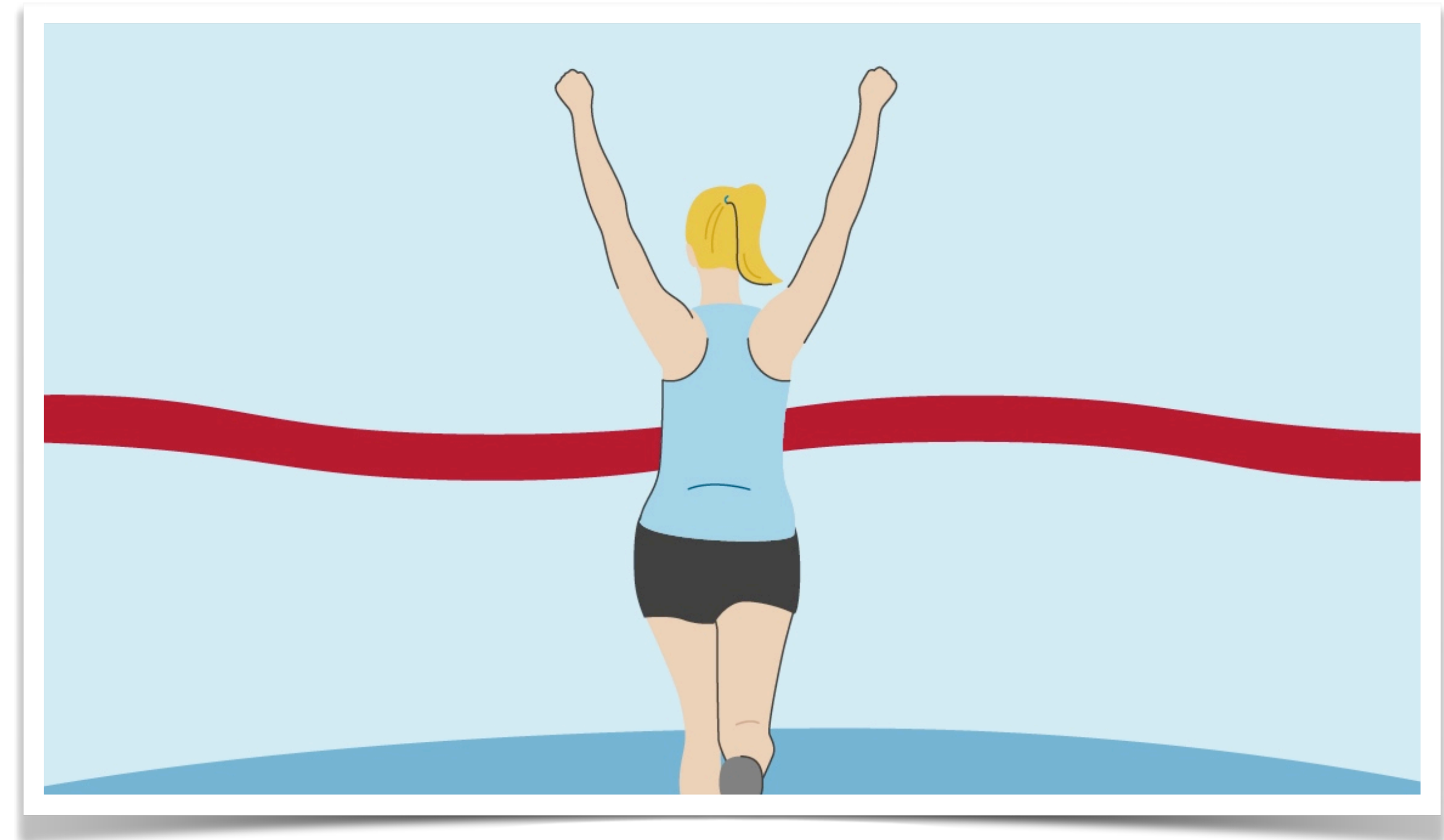
- Small effort more to assess the 32deg analysis normalization
- The systematic errors from detection efficiency and PID selection have to be added to the total systematic error
- Comparison with FLUKA model and other published data can be shown...



# Conclusions

- Small effort more to assess the 32deg analysis normalization
- The systematic errors from detection efficiency and PID selection have to be added to the total systematic error
- Comparison with FLUKA model and other published data can be shown...

...But the analysis is done : )



# Thank you for the Attention

---

(...and the patience...)